RAPID ORBIT REFINEMENT OF POTENTIAL NEAR-EARTH OBJECTS AND RECOVERY OF NEARLY LOST ASTEROIDS

Austin Lantz Caughey

COLUMBUS STATE UNIVERSITY

RAPID ORBIT REFINEMENT OF POTENTIAL NEAR-EARTH OBJECTS AND
RECOVERY OF NEARLY LOST ASTEROIDS

A THESIS SUBMITTED TO
HONORS COLLEGE
IN PARTIAL FULFILLMENT OF THE
REQUIREMENT FOR HONORS IN THE DEGREE OF

BACHELOR OF SCIENCE
DEPARTMENT OF EARTH AND SPACE SCIENCES
COLLEGE OF LETTERS AND SCIENCES

RAPID ORBIT REFINEMENT OF POTENTIAL NEAR-EARTH OBJECTS AND
RECOVERY OF NEARLY LOST ASTEROIDS

By

Austin Lantz Caughey

A Thesis Submitted to the

HONORS COLLEGE

In Partial Fulfillment of the Requirements
for Honors in the Degree of

BACHELOR OF SCIENCE
EARTH AND SPACE SCIENCE, ASTROPHYSICS AND PLANETARY GEOLOGY
COLLEGE OF LETTERS AND SCIENCES

Thesis Advisor _____ Date 7/25/16
Dr. Andy Puckett

Committee Member _____ Date 4/19/16
Dr. Rosa Williams

Honors College Dean _____ Date 4/19/16
Dr. Cindy Ticknor

Abstract

The Minor Planet Center alerts researchers about potential discoveries of new Near-Earth Objects (NEOs) on their NEO Confirmation Page (NEOCP). Most of these are indeed previously unstudied objects, which must be studied very promptly while initial predictions of their motions are still accurate. My thesis project has focused on the observation of these bodies, and the submission of their measured positions to the MPC within a few hours of observation. Data has been obtained using the Skynet Robotic Telescope Network, including the R-COP telescope in Perth, Australia; the PROMPT 3 telescope in La Serena, Chile; and Yerkes Observatory in Williams Bay, Wisconsin. I was also granted access to the private Stone Edge Observatory telescope in El Verano, California. In addition to NEOCP hunting, I have used similar methods to recover previously discovered objects whose predicted positions are becoming so uncertain that without new observations, they will become effectively lost.

Acknowledgements

TABLE OF CONTENTS

Introduction

The orbits of solar system bodies, in particular asteroids and comets, have some amount of uncertainty in their orbits. This is often due to a lack of observations on the object. By observing the object and then measuring its position at a certain time, we refine the object's orbit by making our current understanding more certain and future positions on the object can be more accurately predicted. For things such as trans-Neptunian objects, centaurs, and long-period comets, refining orbits may be purely scientific curiosity. However, Near-Earth Objects (NEOs) and Main Belt Objects pose threats as potential Earth-impactors due to their closeness to Earth. This makes refining orbits and predicting positions of these bodies critical to planetary defense.

A division of the International Astronomical Union (IAU) called the Minor Planet Center (MPC) is responsible for maintaining a list of potential Near-Earth Objects called the NEO Confirmation Page (NEOCP) which is made available online. On this list are objects that are seen by observatories including the Catalina Sky Survey, the Mt. Lemmon Survey, Pan-STARRS, and others who are concerned with NEOs. The NEOCP contains information such as the number of observations on an object, the arc of time across it has been observed, how long it has been since the last observation, and an important parameter called the NEO score. The NEO score is the percentage of current possible orbits that would identify the object as a NEO. That is, how many of the possible orbits put the object within 1.3 AU of the Sun?

Observers are able to choose objects off of this list and observe them in order to refine their orbits. Doing so before the body receives an official designation by the MPC results in publication credit as part of the initial orbit determination team, through co-authorship of a Minor Planet Electronic Circular (MPEC). These MPECs are difficult to obtain due to the rapid nature at which objects are confirmed and removed from the NEOCP.

NEO conformation work is very popular, but often the attention of the astronomy community dissipates once the objects receive official designations. Although their orbits at this point are moderately well-known for the immediate future, orbital uncertainty grows as time passes. This is mostly due to differing semi-major axes in possible orbits and the effect this has on orbital speeds and orbital periods based on Kepler's Laws. Making follow-up observations can further refine that object's orbit and make it certain for longer. If an object does not receive these observations, its uncertainty can grow until it becomes larger than the field of view of our instruments, at which point it can no longer be observed and is deemed lost. We can observe objects, which we call Nearly-Lost Asteroids (NLAs), whose apparent spread in positional uncertainty puts the object in danger of being lost.

This thesis project intends to refine the orbits of five NEOs and two NLAs in order to be more certain about the orbits of these bodies.

Procedures

For our observations, we used a robotic telescope network called Skynet. Skynet offers access to an array of telescopes to students, educators, and professional astronomers. Observers are able to submit observation requests to the desired telescope over the Internet, to be completed as soon as possible. Images are then downloaded from the website and subsequent image analysis occurs by the user. The telescopes we used for this project are Yerkes Observatory (observatory code 754) in Williams Bay, Wisconsin, USA; the R-COP telescope (323) in Perth, Australia; and the PROMPT 3 telescope (807) in La Serena, Chile. I was also granted access to the private Stone Edge Observatory (G52) telescope in El Verano, California.

Skynet makes observing asteroids with official designations, including NLAs, or other bodies such as nebulae or galaxies relatively simple. Inputting the object's designation allows Skynet to access an ephemeris created from observations in the Minor Planet Center Orbit Database (MPCORB)[1] in order to predict the position of the object at any given time in the future.

Objects with no official designation are quite different. With these objects, Skynet cannot access an ephemeris on its own. The user must plan the observation for a certain time range and then enter the right ascension and declination coordinates manually so that the object will actually be in the field of view of the telescope. [1]Multiple observations of the same type at different times may be required to ensure the images needed are obtained. The NEOCP website allows users to create an ephemeris that can be used for this purpose by simply selecting the desired NEOCP object, entering an observatory code, and selecting a time interval. However,

---

[1] Minor Planet Center, 2016, MPCORB, International Astronomical Union, http://www.minorplanetcenter.net/iau/MPCORB.html

these ephemerides are only accurate for a short time interval, due to the lack of observational data on these objects, and must be obtained quickly.

Once the object and its position are selected and input into Skynet, additional information is required before the observation can be queued. First, a telescope must be chosen. We primarily used the R-COP telescope in Western Australia and the Yerkes Observatory in southern Wisconsin. Although its small 14-inch aperture limits its abilities as a powerful telescope, R-COP is convenient because it is on the other side of the world, which allows real-time observing to be done during the day time. Yerkes is ideal because of its large light-collecting power thanks to its 40-inch diameter primary mirror. The Prompt telescopes are placed on a mountaintop in Chile; this means very little light pollution and less airmass to see through.

Second, a filter must be chosen. For many astronomical studies, light is filtered out in order to study a single range of wavelengths. This allows astronomers to gain important information regarding the flux density in certain bandpasses which can help determine other physical characteristics about the object. For our purposes, we need as much light as possible in order to actually detect the object. Selecting a "Maximum Light" filter such as Open, Clear, or Lum will allow most wavelengths of light to pass through to the detector.

Lastly, Skynet needs imaging instructions, including the length of the exposures and how many the observation requires. Since imaging NEOCP objects through Skynet requires locking on to a star field instead of tracking the objects, the asteroid may leave the field of view of the telescope. Because of this, it is advised that you set an expiration date for your observation. Once this information is entered, Skynet will present a final confirmation page. By clicking "Submit", the observation request is officially placed in the observatory's queue and will be taken when weather and the observation's place in the observing queue permits.

As each image is taken, it is available for download. One of the many great things that Skynet does is automatically apply calibration frames to each images. These calibration frames biases, darks, and flats correct for electronic noise in the detector, thermal noise, and consistent detector response and flaws in the optical path, respectively. Having these applied automatically saves a great deal of time and greatly helped my measurements be done in a timely manner.

Astrometrica

Once the observation is complete and the images are downloaded, software called Astrometrica is used to make measurements of an image in RA-Dec coordinate space. It is particularly useful because it can access MPC data and predict positions of known asteroids. Another useful function is its "Track and Stack" capabilities, which allow us to stack images using the apparent motion vector, called the proper motion vector, of the object in question. This results in a brighter image of the asteroid, while the starlight is spread out as streaks in the final stacked image. Typically, a set of observations would be split into three image stacks, which allows the motion of the asteroid to be confirmed, while also allowing for the largest number of images to be used in each stack. In a single image, there would be no observable difference in an asteroid or star apart from the point-like appearance of the asteroid in contrast to the streaked appearance of the stars. Of course, no motion can be confirmed in a single image. In two images, noise can easily be misidentified as a moving signal source. In three images, any consistent motion would very likely be a moving signal source, such as a minor planet. The images used to make measurements on each object can be found in Appendix A.

Find_Orb

Once measurements are made, we decided to quantify whether or not we actually improved the knowledge of the object's orbit. To do this, we use an astrostatistical software

called Find_Orb. This software can take input a list of existing observations for an object and solve for a best-fit orbit. It also lists the mean residual of the measurements and the individual residuals of each measurement. By observing the change of the individual uncertainties in each orbital parameter and comparing the residuals of our measurements to those of previously existing ones, we can quantify whether we have aided the object's orbit or if the measurements are faulty or need better precision. See Appendix B for Find_Orb information for each object.

We also use Find_Orb's Monte Carlo function to generate multiple possible orbits. Monte Carlo is a statistical method that randomly generates an outcome within certain bounds (Metropolis, Ulam, 1949). By using this multiple times, we can model the uncertainty in a minor planet's orbit, as discussed below.

OrbitMaster

Another way to see how our measurements improve the orbit of an object is by modelling the uncertainty of the orbit. For this we use OrbitMaster, a variation of the OrbitViewer Java applet found on the Jet Propulsion labs website, which has been adapted by Dr. Andy Puckett to serve our purposes (Puckett, 2016). OrbitMaster can take an input orbit for an object and display it in three dimensions. It also has the ability to play, fast-forward, and rewind time which allows the user to see how the object's position changes over time according to Kepler's Laws. OrbitMaster is actually most useful for highly uncertain objects with multiple possible orbits. In order to visualize these uncertainties, we use Find_Orb to create usually hundreds of possible orbits using its Monte Carlo function. These orbits are saved and input into Orbit Master for display. This combined with the ability to manipulate time allows us to see how the uncertainty in position changes over time.

Results and Interpretations

<u>NEOCP Objects</u>

P10rRRx (2016 BD$_{39}$)

During the morning of 2016 February 2, I attempted to refine the orbit of NEOCP object P10rRRx. I submitted the observation request to R-COP and watched as the images were taken in real-time. Immediately after the observation was completed, I began analysis on the images. In order to stack the images, a proper motion vector from the NEOCP website was needed. I then went back to the page, only to find that the object had been taken off and given an official designation while the analysis was taking place. This shocking and disappointing find only highlighted the fact that NEOCP objects need to be selected carefully and their measurements submitted rapidly. Even though our work wasn't included in the discovery MPEC, our observations were the first to be received by the MPC after its publication. According to the OrbitMaster visualizations in Figure 11, my observations still contributed significantly to reducing the uncertainty even though my work was not submitted quickly enough for the MPEC.

The object was rather faint and at the moderate speed of 2.073 "/min, 59 images of 60 second exposures wasn't enough to see it more in more than one stacked image. To remedy this, we submitted observations for a second night on R-COP the next day. By this time, the object was moving at 2.028 "/min and was in a totally different starfield (see Figure 1). Now with two sets of around 60 images at 60 seconds of exposure time, both sets of observations were stacked for two stacks composed of 60 frames each. Using an ephemeris generated by Find_Orb, the general region in where to look for the asteroid was known. I made the measurements and submitted them to the Minor Planet Center.

XD26E1F (not confirmed)

One of the risks of attempting to confirm these newly "discovered" and rarely observed objects is that the object might not exist at all. Noise in an image sequence can easily be mistaken as an actual object if the "motion" of the noise in the images is consistent. Perhaps the best way to debunk whether or not the object is real is to obtain more observations on the object, which is why the NEOCP exists.

On 2016 February 18, I submitted an observation request to Yerkes for the NEOCP object XD26E1F. The NEOCP listed its apparent magnitude at 20.7, so my observation request consisted of 60 images at 60 seconds each. The object was moving at the moderate speed of around 4.5 "/min. These observations occurred during the asteroid's close approach with the Earth; the fastest speed in the ephemeris was 4.54 "/min at around 08 UT. The observations were perfect and the images aligned very nicely. The problem was that I could not locate the object in the images. I even went so far as to interpolate the proper motion values to coincide with the middle time of the images stacked for input into the Track and Stack procedure. Still, the object was not found. On February 23.75 UT, the object was removed from the NEOCP, with the MPC claiming that the object "was not confirmed". This essentially means the object did not exist. This outcome is common for NEOCP objects and was not surprising. As shown in Table 2, the object had not been seen for over a day and lacked many observations which is a sign that the object may be problematic. While initially disappointing, these disconfirmations are equally as important as confirmations.

XC85137 (2016 CL₁₃₇)

These observations consisted of 71 images, though 80 were requested. This is due to a small "competition" with another Skynet user. As is expected in a queue-based telescope system, there were scheduling conflicts. When this occurs, the user whose observations are of higher priority will be taken first. In this case, my low priority observations were trumped by a higher priority observation midway through my observations. Although they were never completed, the observation sets contained enough images to make reasonable detections of the objects. The lesson to be learned here is that telescope time is precious and one's observations may not be completed. The observer should be prepared for this to occur and be flexible in their preparations that reasonable measurements can be obtained should this happen. The objects affected were XC85137, XC83AD6, and XC20069.

As shown in Tables 3 and 4, the object XC85137 had a NEO rating of 100%, before and after our observations, which makes it a prime candidate for this type of research. The object was moving with a proper motion of 3.74 "/min, which is moderate for NEO objects. The images were taken by R-COP on February 9, 2016 at around 15:30 UT. Data reduction forced twelve images to be removed from the set. Although these images were clearly the same starfield, Astrometrica would not align the images properly. This error was actually quite common amongst all R-COP observations. This forced us to use four stacks instead of three to use all of our images, as shown in Figure 2. They were stacked with 24 frames in the first two images, eleven in the third, and twelve in the last. At an exposure of 45 seconds per frame, this gives the stacked images times of eighteen minutes, eighteen minutes, 8.25 minutes, and nine minutes on the object, respectively. The object was found in the images, and the measurements were submitted to the MPC in time (Caughey et al., 2016-C129).

In order to truly gauge the effectiveness of these observations, I created OrbitMaster visualizations for each step in the orbit refinement process as shown in Figure 13. The first image shows the radical uncertainty in the object's orbit. It even shows that the object had the possibility to be a Trans-Neptunian Object. It was created from observations than spanned only 4.8 hours. The second visualization includes my observations, which *greatly* reduce the uncertainty and essentially confirm the object to be a NEO. My observations stretched the observation time to nearly eleven hours. Another large factor that contributed to the uncertainty reduction was the fact that all prior observations were from telescopes in Arizona, while my observation were from Australia. This large baseline allows a quasi-parallax effect that more accurately determines the object's distance from the Earth.

XC83AD6 (2016 CD$_{137}$)

This target was chosen because its relatively low NEO rating of 77% (see Table 6) presented the opportunity to observe a possible NEO that might get passed by other astronomers since there is a lesser chance of an MPEC. Of the three objects observed on 2016 February 9, this one was the fastest at 5.33 "/min. It was quite faint at an apparent magnitude of 19.9. The observation was intended to consist of 120 images of 30 seconds of exposure time. However, due to the aforementioned issues with this set of observations, only 113 were obtained. In this set, nine images were of poor quality. These were removed , resulting in a total of 104 images. These errors are the same as the errors that were in the XC85137 observations. As shown in Figure 3, the stacks contained 36, 29, and 39 images, respectively. The object was found in the images and submitted to the MPC. I was successful in my attempts and was published in MPEC 2016-C120 (Caughey et al., 2016).

XC20069 (2002 TT$_{206}$)

I selected the object XC20069 due to its high brightness and relatively low NEO rating of 75% (see Table 8). I was extremely timely in my study of this object, as my observations were taken a mere seven hours after the Catalina Sky Survey first discovered the object. The images were taken using R-COP on February 9, 2016. Table 8 shows the information necessary to schedule the observations and stack them properly. The object was moving extremely slowly for a NEO at only 0.36 "/min, which might bring into question the object's potential classification as a NEO. The observation request was for 60 images of 60 second exposures. However, due to the previously mentioned conflicts with higher priority observations, only 36 images were obtained. Thankfully, this was still sufficient to see the object in the images with reasonable signal-to-noise ratio (SNR). These images were split evenly into three stacks containing twelve images. The object was barely detected with a SNR of around 3.4. Once my measurements were submitted, the object's NEO rating dropped tremendously from 75% to 43% as shown in Tables 8 and 9. The MPC later linked the NEOCP measurements to a previously discovered object 2002 TT$_{206}$. Recoveries of previously-known objects do not get published in the MPECs, but my work on this object was published in the Minor Planet Circular 97718 (Biggs et al., 2016).

The Find_Orb and OrbitMaster analysis for this object was quite a challenge. When I observed XC20069, the only other existing observations were the discovery observations (4 measurements over 42 minutes) from the Catalina Sky Survey. This lack of observational data led to difficulties while attempting to generate reasonable alternate orbits with Find_Orb using the Monte Carlo method. Luckily, I managed to get the file containing alternate orbits generated by the MPC with an appropriate OrbitMaster visualization could be created. Their method of calculating these orbits is quite different from the Monte Carlo method we have been using.

While this allowed me to make a visualization for the state of the object before my

measurements, I did not manage to obtain the MPC's alternate orbits file for the state of the

object with my added observations. I ran into an issue with lack of data for the Monte Carlo

process. To remedy this, I added measurements from Haute Provence (511) located in southern

France, which came directly after my measurements, and used the Vaisala orbit solution method.

Vaisala is a method that assumes the object is at perihelion or aphelion (distance in AU is input

manually), takes the first and last observation in a list of measurements, and fits them to an orbit.

Although this is an unreliable long-term orbit determination method, the assumptions made

about the orbit are reasonable enough to predict the positions over the course of few days.

Luckily, I used Vaisala at a time in the future in which the perihelion/aphelion values were

known which allowed me to run Find_Orb analysis shown in Figure 16. Following the Vaisala

with the standard 500 Monte Carlo orbits produced an OrbitMaster visualization that shows

orbits that are tweaked around the best-fit orbit for the Vaisala. Unsurprisingly, the visualizations

showed a significant decrease in uncertainty compared to the initial orbits obtained from the

MPC's alternate orbits file which can be seen in Figure 17.

XC1EF0C (2016 CH$_{137}$)

On 2016 February 10, frequent collaborator Vivian Hoette sent me information regarding

NEOCP object XC1EF0C. She used the private Stone Edge Observatory (SEO; G52) in El

Verano, California to observe this object. My job was to download the images and make the

necessary measurements. The observation set contained 120 images with exposure times of ten

seconds each, which allowed for 3 stacks of 40 images as shown in Figure 5. The predicted

magnitude was 20.3, which is on the faint side of objects for SEO but still reasonably bright for

the NEOCP. The MPC ephemeris also gives a speed of around 8.8 "/min, which is pretty fast for NEOs.

The images were stacked, but the object did not appear to be in the images. Upon realization that since Stone Edge is not on Skynet the images were not automatically calibrated, I manually applied the available darks. This was done in Astrometrica because of the simplicity of applying them. The user simply selects each of the calibration frames to be used and any images opened after selecting the calibration frames will be fixed by the software. Applying the calibration frames got rid of some electronic noise from dark current. This allowed the object to be seen more clearly and be measured with a reasonable SNR at around 6 (see Table 11). The measurements were submitted and were published in the MPEC 2016-C124 (Gilmore et al., 2016.

XC22469 (2016 CM$_{194}$)

On 2016 February 12, Vivian Hoette sent me another set of Stone Edge observations to analyze, this time of NEOCP object XC22469. The observation set contained 33 images with exposure times of ten seconds, which allowed for three stacks of eleven images each. The object was very bright for an undesignated asteroid with a predicted magnitude of 17.7, but was moving extremely quickly at around 17.8 "/min which can be seen in Figure 6. This rapid movement and the brightness of the object explain the brief exposure times. Once the images were stacked, with the proper calibration frames applied, the object was easily spotted and measured. The measurements had outstanding SNRs of around 17-19 as shown in Table 12. The measurements were submitted and published in MPEC 2016-C160.

The OrbitMaster visualization for this object shows something very interesting; a close approach with the Earth (see Figure 21). According to the Minor Planet Ephemeris Service, on

2016 February 13 at around 8 UT, XC22469 came within 0.00052 AU to the Earth, which is only

20% of the mean Earth-Moon distance. If the object had been larger, it would have been a

Potentially-Hazardous Asteroid (PHA). These objects must have an Earth MOID of less than 20

lunar distances and an absolute magnitude brighter than 22, which is the best indicator of size

that we have for these objects. Thankfully, this object only had an absolute magnitude of 27.8

which relates to a diameter of around 10 m or 11 yards (CITATION FOR NASA NEO THING).

The gravitational interaction resulting from this close approach perturbed the orbit of the

asteroid, causing problems with Find_Orb's calculations of alternate possible orbits, which were

exacerbated by the relative lack of observational data. My solution was to eliminate all

observations near and after the close approach which can be seen in Figure 20. This allows me to

more reasonably compare the effect my observations had on the orbit with the final state of the

orbit before the close approach.

P10sJtm (2016 CO$_{264}$)

This situation was particularly interesting. Our friend and colleague Vivian Hoette, the

Director of Special Projects at Yerkes Observatory, sent us a set of observations taken from

Yerkes for the NEOCP object P10sJtm. All observations and measurements went according to

plan and our measurements were submitted within 24 hours after receiving the observations. Our

measurements were accepted and added to the NEOCP's list of observations, but the object was

not granted an official designation within the usual timeframe. It was moved to the Potential

Comet Confirmation Page (PCCP) most likely due to the orbit being foreseen by the MPC as a

long-period orbit. It stayed on the PCCP for over two weeks, rarely observed over that span of

time, awaiting confirmation of cometary activity (which never came). Therefore, the object was

designated as asteroid 2016 CO$_{264}$ in MPEC 2016-D46, crediting our work.

Find_Orb and OrbitMaster analysis, Figures 22 and 23 respectively, showed that the report of cometary activity might not have been unreasonable. The final nominal orbit for this object has a semi-major axis of around 49 AU and an orbital period of 334 years. The orbit stretches from perihelion in the Main Belt, to aphelion well beyond the Kuiper Belt, effectively designating this as a Trans-Neptunian Object (TNO). When TNOs have very eccentric orbits such as this, they are usually long-period comets. Based on this, I suggest that the report of cometary activity was actually quite reasonable.

NLAs: Nearly-Lost Asteroids

2012 SZ$_{58}$

This object was an NLA that was in danger of becoming lost. Its orbit at the time of our observations was based on 47 measurements over 78 days in 2012. It had not been observed since 2012 December 14. We used R-COP to observe the object on 3 February 2016. At around 20th magnitude, it was around average brightness for these objects. The body moved at 0.572 "/min, a slow speed which was expected from a Main Belt, non-NEO object. Since the object could be detected with a respectable signal-to-noise ratio (average 4.4, see Table 15) with only ten images in a stack, we created six stacks and made six measurements. The measurements were submitted and accepted which resulted in our work being published in MPC 97718 (Biggs et al., 2016). The best indicator of the effect of our observations is the OrbitMaster visualization in Figure 25. The increasing uncertainty in the object's predicted position would have led the object to become lost over time. Subsequent observations even further reduced that uncertainty. The object's position will be accurately predictable for a long time.

2012 BC₃

On 2016 February 4, our first useful image sequence was obtained for asteroid 2012 BC₃. This object had been discovered in 2012 but had not been seen since 2014, which made it an excellent candidate for NLA orbit refinement. Dr. Puckett first attempted to image this asteroid using the R-COP telescope on February 2, but the images were not useful due to a poorly-placed star. Our close collaborator, Tyler Linder, then took sixty 20-second images of the object on February 4 using Skynet's PROMPT 3 telescope in La Serena, Chile. When these images were finally analyzed a month later, the object was difficult to spot due to its low proper motion and relative faintness (0.472 "/min and 20th magnitude, respectively). This difficult detection would need to be confirmed with a second night of observations, as required by the MPC, so we could be sure that the object we found was, in fact, 2012 BC₃.

It was observed again with the Yerkes telescope on 2016 March 7. The observation was supposed to contain 60 images of 60 seconds of exposure time, but cloudy skies only allowed 39 images to be taken. The object was, again, moving rather slowly at only 0.534 "/min. By this time the object had gotten much fainter at magnitudes around 22, which is on the brink of being undetectable. Measurements from both nights were submitted to the MPC and later published in Minor Planet Circular 98868 (Buie et al., 2016).

The OrbitMaster visualizations in Figure __ show a change similar to that of 2012 SZ₅₈. Perhaps the most impressive change is found from the object's greatest peak uncertainty from ASTORB[2]. Before our observations, the greatest peak uncertainty was 96" on 30 March 2025. With our observations, it was reduced to 3.8" on 31 March 2025.

---

[2] E. Bowell, 2016, ASTORB, Lowell Observatory, http://www.naic.edu/~nolan/astorb.html

Conclusions

Over the course of a few months, we refined the orbits of seven NEOCP objects and two NLAs. This resulted in five MPEC publications acknowledging our contribution as part of the initial orbit determination teams for each newly-confirmed NEO. In addition to the observations and measurements which are the core of this type of work, I also analyzed the effectiveness of my measurements at refining the objects' orbits. In one case, an exotic path through the outer Solar System was corrected into a more routine Main-Belt orbit. In other cases, an uncertain position along a fairly well-known orbital path was simply snapped back into certainty. Changes in the uncertainty of the semi-major axis and increase of the arc of observations is shown in the table below. Similar work is done by professional astronomers at several sky surveys and other NEO services.

Object	Uncertainty in Semi-Major Axis (AU)			Arc of Observations (Days)		
	Before	During	Now	Before	During	Now
P10rRRx	±0.0191	±0.0105	±0.000105	3.11946	4.24254	43.70815
XC85137	±1.15	±0.0151	±0.00326	0.18483	0.45206	3.11353
XC83AD6	±0.00019	±0.000177	±4.39E-5	1.05330	1.38915	10.45664
XC20069	n.a.	n.a.	±2.24E-7	0.02913	0.33689	4907.14253
XC1EF0C	±0.00651	±0.00511	±0.0038	1.00592	1.10359	3.9589
XC22469	±0.00332	±0.00216	n.a.	0.15941	0.17300	0.966013
P10sJtm	±0.943	±0.89	±0.488	40.792454	40.92046	81.863833
2012 SZ$_{58}$	±1.64E-5	±2.43E-6	±1.34E-6	78.799839	1226.47368	1262.15257
2012 BC$_3$	±2.41E-5	±6.95E-7	±6.95E-7	973.13215	1534.71406	1534.71406

Perhaps the most important reason this type of work is done on a large scale is because the implications that some of these objects could be potentially hazardous. In order to gauge how close these objects actually come to Earth, we must have a good idea of their orbits. By reducing the uncertainty in an orbit to the point where the orbit is well-understood, we can be sure if a body falls within the parameters that define it as a potentially hazardous object and better prioritize our observations.

This work is also important because of the impact it could have on potential future studies of these bodies. Recent in-depth studies of minor planets include spectroscopy, photometry, and surficial profiles using radar. In order to point our instruments at the object to do this work, the object's orbit must be very well known.

Appendix A: Data and Images for Each Object

P10rRRx (2016 BD$_{39}$)
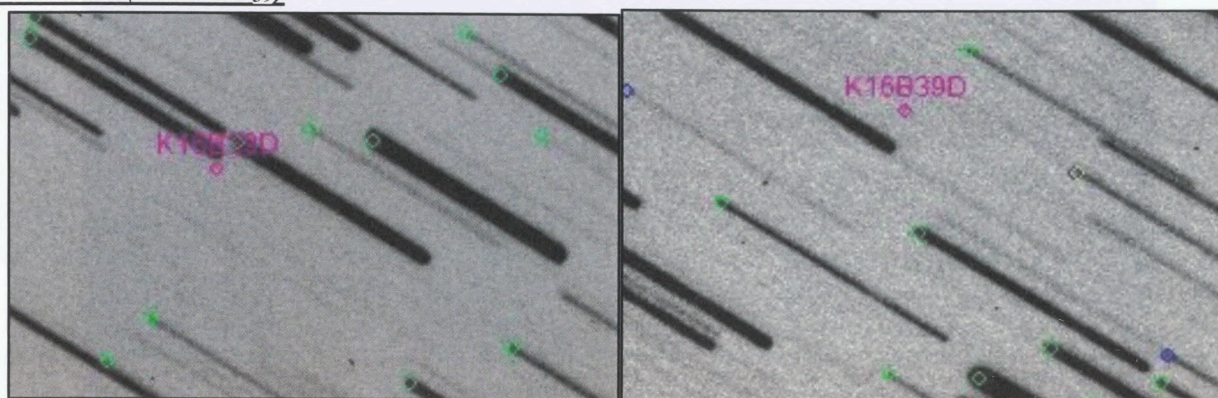
Figure 1: Images of P10rRRx. The observations took place on different days which leads to a change in background stars.

Table 1: Measurement Data for P10rRRx			
Measurement	V	SNR	FWHM (")
1	19.4	4.5	1.4
2	20.7	3.5	2.7

XD26E1F

Table 2: NEOCP Data for XD26E1F at 11:06am on Feb/17/2016									
Score	Discovery	R.A.	Decl.	V	Updated	NObs	Arc	H	Not Seen/days
98	2016 02 16.3	10 31.4	+27 52	20.6	Updated Feb 16.75 UT	10	0.10	26.4	1.197

XC85137 (2016 CL₁₃₇)
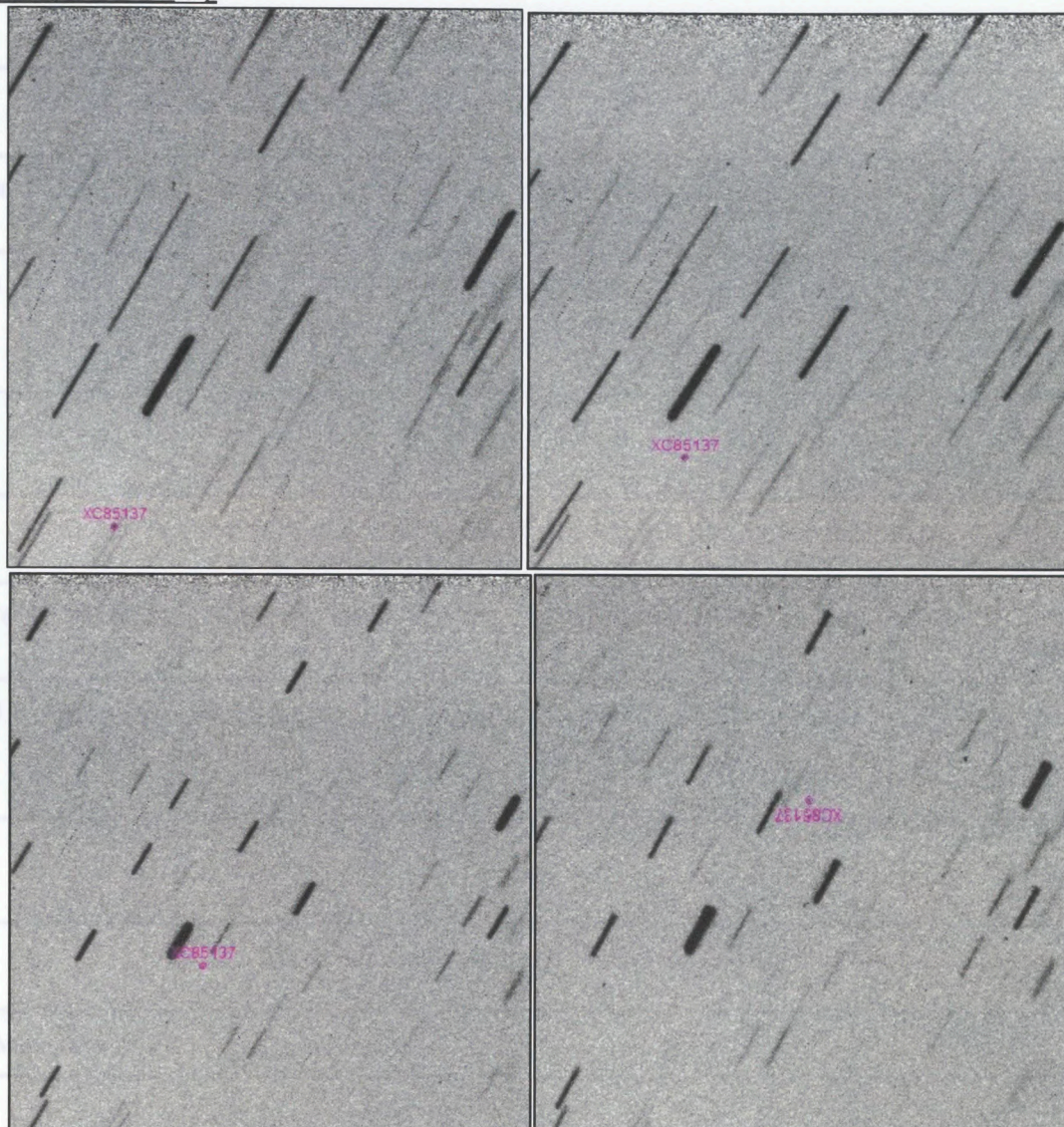
Figure 2: Stacked images from the XC85137 observation set. Images are in chronological order from top left, to bottom right. This demonstrates a motion to the top right of the field of view. XC85137 at 10:55am on 2016 February 9

Table 3: NEOCP Data for XC85137 at 10:55am on Feb/9/2016									
Score	Discovery	R.A.	Decl.	V	Updated	NObs	Arc	H	Not Seen/days
100	2016 02 09.4	09 16.0	+12 27	19.5	Updated Feb 9.46 UT	16	0.18	25.7	0.216

Table 4: NEOCP Data for XC85137 at 10:32pm on Feb/9/2016									
Score	Discovery	R.A.	Decl.	V	Updated	NObs	Arc	H	Not Seen/days
100	2016 02 09.2	09 15.0	+12 59	19.9	Updated Feb 9.92 UT	20	0.45	25.7	0.427

Table 5: Measurement Data for XC85137			
Measurement	V	SNR	FWHM (")
1	20.2	7.2	1.5
2	20.4	4.1	1.7
3	20.1	4.0	1.4
4	19.1	5.9	0.8

XC83AD6 (2016 CD$_{137}$)
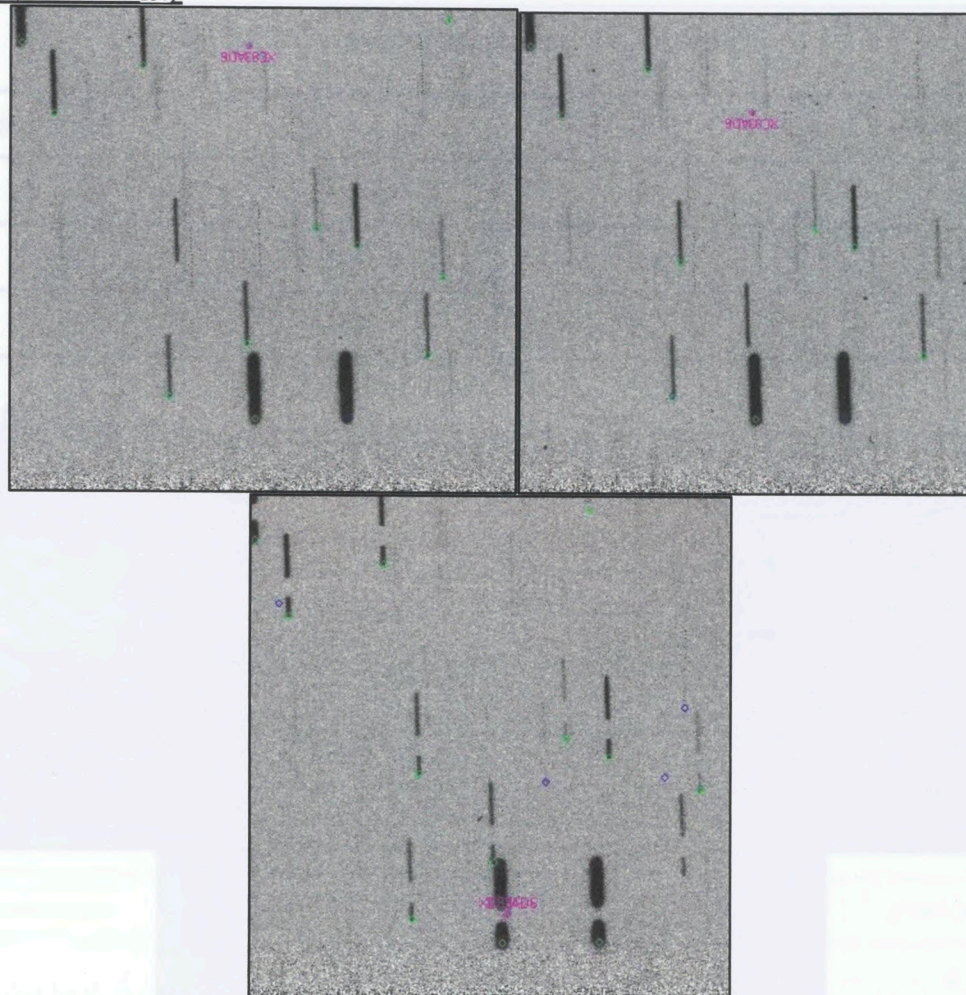
Figure 3: Stacked images of XC83AD6. In chronological order, motion is nearly vertical, which is actually in the negative Declination (δ) direction.

Table 6: NEOCP Data for XC83AD6 at 10:55am on Feb/9/2016									
Score	Discovery	R.A.	Decl.	V	Updated	NObs	Arc	H	Not Seen/days
77	2016 02 08.3	09 51.2	+17 12	19.9	Updated Feb 9.60 UT	31	1.05	26.1	0.248

Measurement	V	SNR	FWHM (")
1	20.4	5.1	1.6
2	19.4	6.0	1.6
3	19.3	6.1	2.8

Table 7: Measurement Data for XC83AD6

XC20069 (2002 TT₂₀₆)
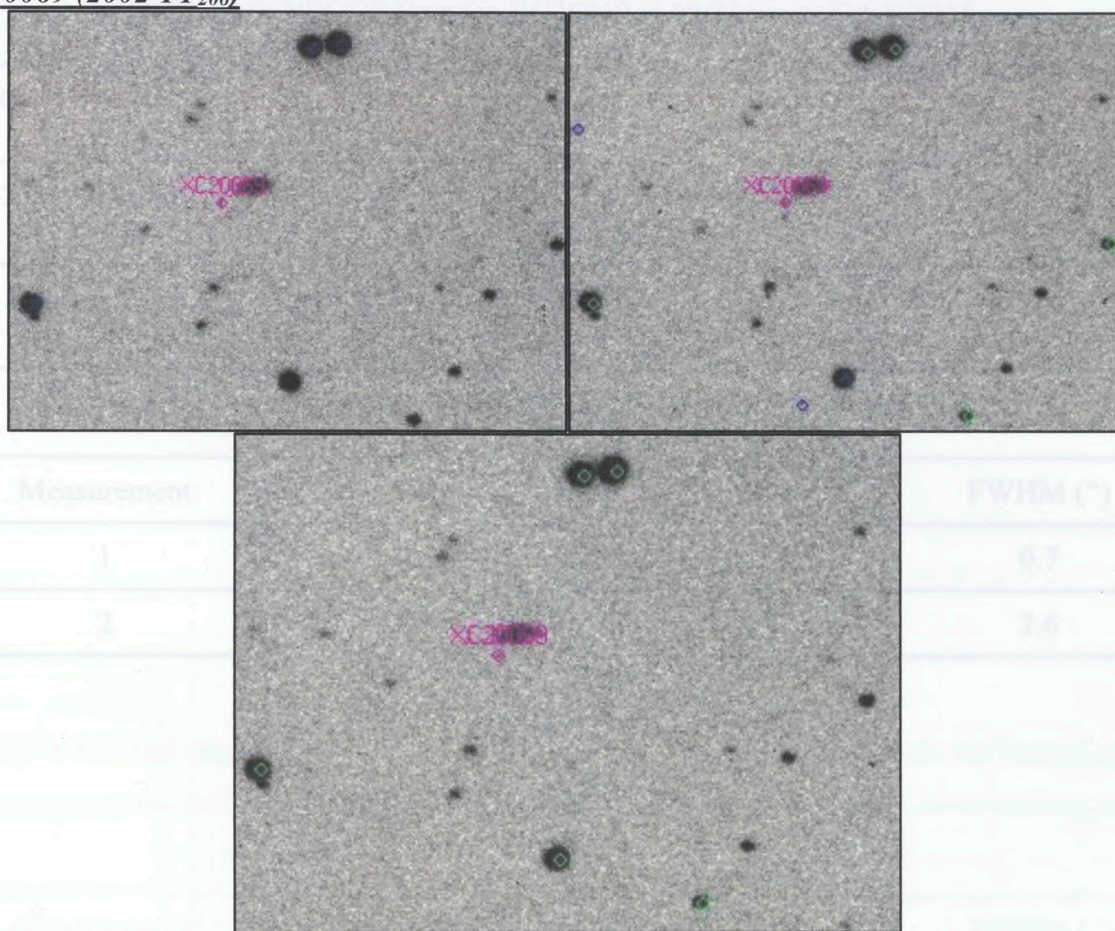
Figure 4: Stacked images of XC20069. Although it is extremely slow, the motion can be seen progressing towards the bottom left.

Table 8: NEOCP Data for XC20069 at 10:55am on Feb/9/2016									
Score	Discovery	R.A.	Decl.	V	Updated	NObs	Arc	H	Not Seen/days
75	2016 02 09.4	13 14.8	+22 40	19.9	Added Feb 9.55 UT	4	0.03	17.4	0.135

Table 9: NEOCP Data for XC20069 at 10:34pm on Feb/9/2016									
Score	Discovery	R.A.	Decl.	V	Updated	NObs	Arc	H	Not Seen/days
43	2016 02 09.4	13 14.4	+22 40	19.9	Updated Feb 9.95 UT	6	0.34	17.4	0.306

Table 10: Measurement Data for XC20069			
Measurement	V	SNR	FWHM (")
1	19.7	5.8	0.7
2	19.4	3.4	2.6

XC1EF0C (2016 CH₁₃₇)

Figure 5: Stacked images of XC1EF0C. The motion of the asteroid is towards the bottom right of the field of view.

Table 11: Measurement Data for XC1EF0C

Measurement	V	SNR	FWHM (")
1	19.8	10.5	6.5
2	19.8	14.2	4.0
3	19.5	8.1	6.0

XC22469 (2016 CM194)
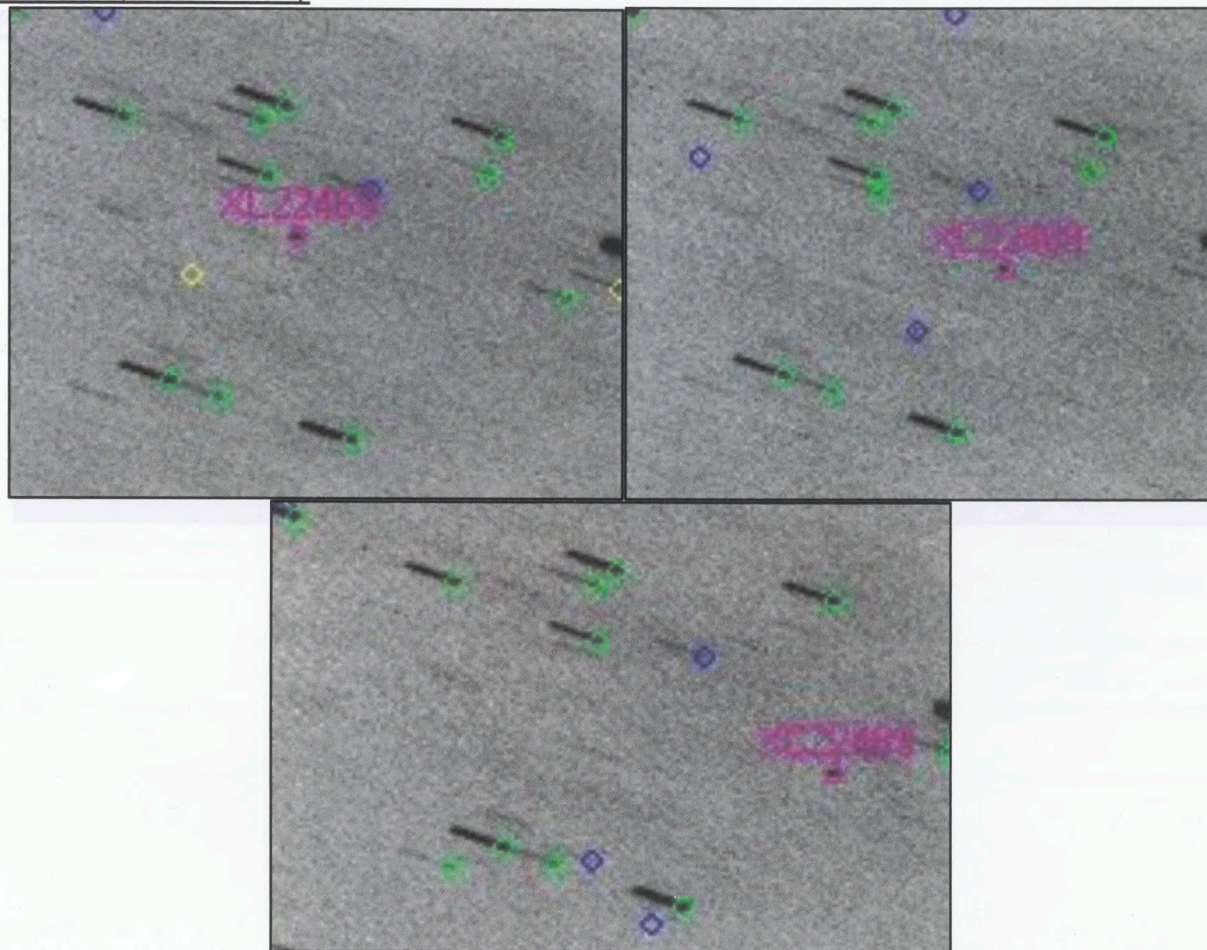
Figure 6: Stacked images of XC22469. The object's motion is towards the bottom right.

Table 12: Measurement Data for XC22469					
Measurement	V	SNR	FWHM (")	"/min	PA
1	17.8	19.0	4.4	17.73	251.0
2	17.9	16.8	5.1	17.82	250.8
3	17.9	18.2	4.9	17.95	250.5

P10sJtm (2016 CO₂₆₄)
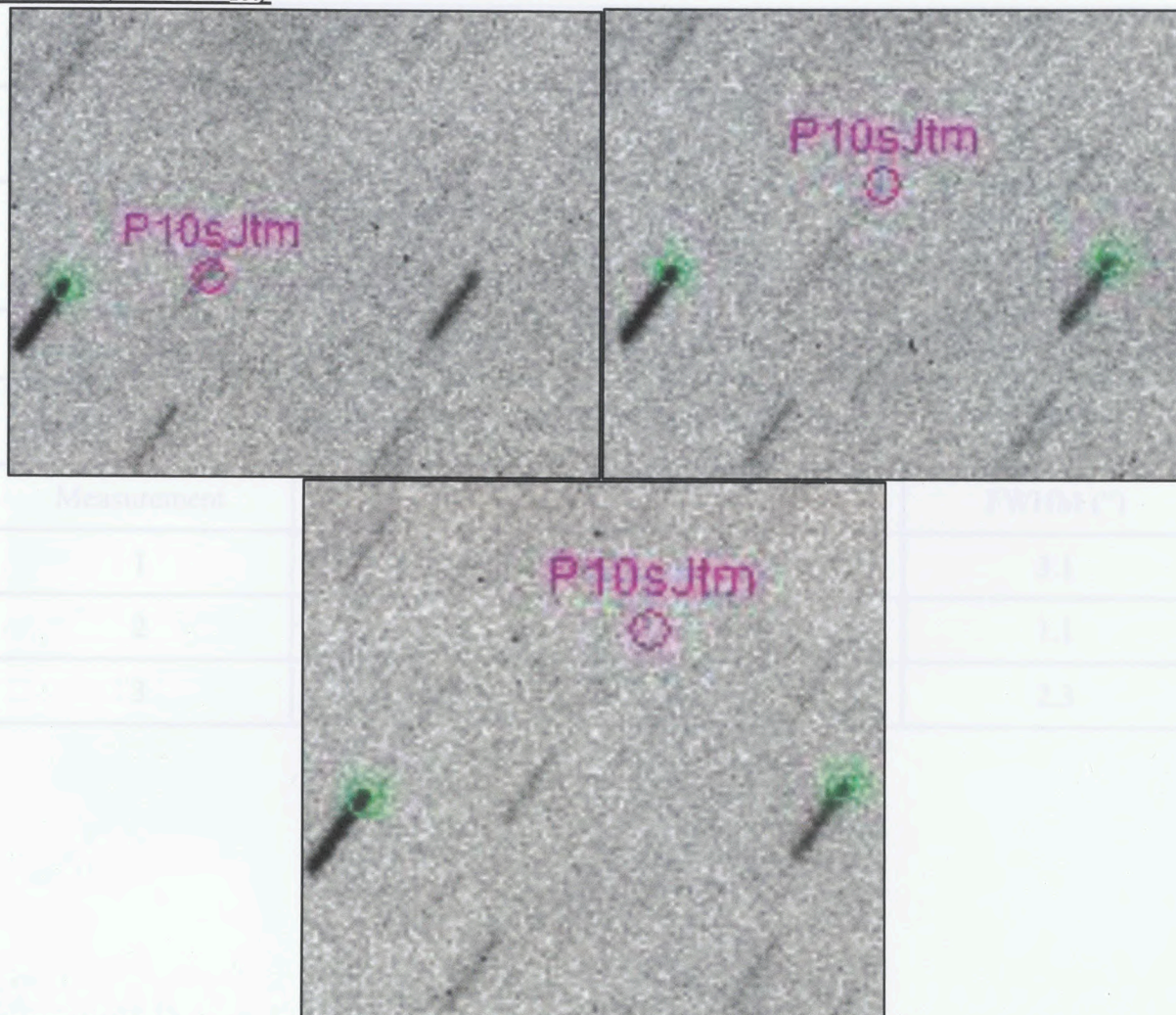
Figure 7: Stacked images of P10sJtm. The object's motion is to the top right of the field of view.

Table 13: NEOCP Data for P10sJtm at 3:40pm on 17 Feb. 2016									
Score	Discovery	R.A.	Decl.	V	Updated	NObs	Arc	H	Not Seen/days
98	2016 02 16.3	10 30.5	+28 06	20.6	Updated Feb 17.75 UT	10	0.10	26.4	1.362

Table 14: Measurement Data for P10sJtm			
Measurement	V	SNR	FWHM (")
1	20.5 (in front of star)	8.9	3.1
2	22.0	7.0	1.1
3	22.0	6.6	2.3

2012 SZ₅₈

Figure 8: Stacked images of 2012 SZ₅₈

Table 15: Measurement Data for 2012 SZ_{58}			
Measurement	V	SNR	FWHM (")
1	20.2	4.7	1.1
2	20.2	4.0	2.4
3	20.1	3.8	2.1
4	20.0	5.5	2.3
5	20.2	4.9	1.6
6	20.1	3.5	2.1
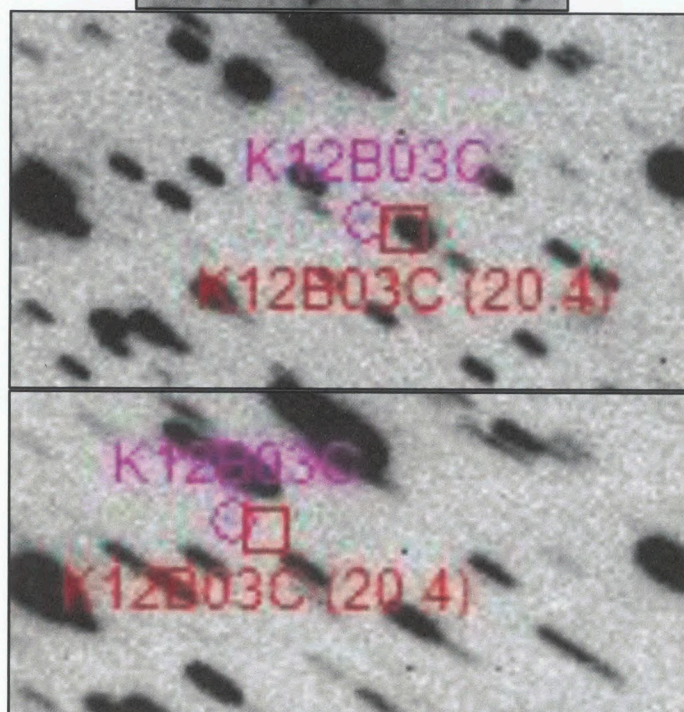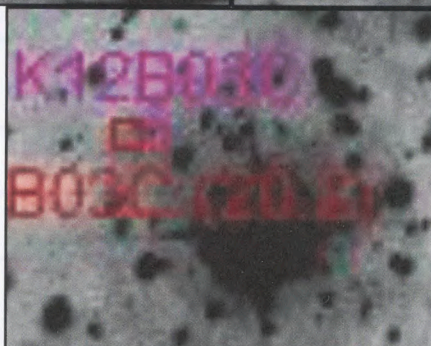
2012 BC3

Figure 9: Stacked images of 2012 BC₃. The first two rows are from Yerkes and the last row is from Prompt-3.

Table 16: Measurement Data for 2012 BC3			
Measurement	V	SNR	FWHM (")
Prompt-3 Measurements			
1	19.9	6.8	3.1
2	20.3	7.6	2.9
3	20.5	6.4	2.8
Yerkes Measurements			
1	22.3	6.4	3.2
2	22.9	6.2	3.3

Appendix B: Find_Orb Data and OrbitMaster Visualizations for Each Object

P10rRRx (2016 BD39)

```
Orbital elements: P10rRRx
  Perihelion 2016 May 8.601657 +/- 0.752 TT = 14:26:23 (JD 2457517.101657)
Epoch 2016 Feb 2.0 TT = JDT 2457420.5 Earth MOID: 0.3315 Ve: 0.0660
M 299.25929 +/- 0.8                 Find_Orb
n  0.62877501 +/- 0.0134     Peri. 324.44844 +/- 0.22
a  1.34939531 +/- 0.0191     Node 277.36770 +/- 0.33
e  0.5410869 +/- 0.00861     Incl. 35.13051 +/- 1.8
P  1.57/572.53d       H 20.1  G 0.15  U 9.8
q 0.61925516 +/- 0.00284   Q 2.07953546 +/- 0.0402
From 12 observations 2016 Jan. 30-Feb. 2; mean residual 0".14

1601 30.32211   F51   05 22 15.728   -03 54 59.03   .06+   .12+
1601 30.34872   F51   05 22 10.775   -03 55 46.71   .04+   .04-
1601 30.36203   F51   05 22 08.290   -03 56 10.43   .15-   .01-
1602 01.06386   807   05 17 09.55    -04 45 32.7    .14+   .08+
1602 01.06667   807   05 17 09.05    -04 45 37.8    .10+   .21-
1602 01.06934   807   05 17 08.57    -04 45 42.3    .01-   .15-
1602 01.42478   474   05 16 07.88    -04 55 44.1    .19+   .12+
1602 01.42831   474   05 16 07.25    -04 55 50.1    .05-   .10+
1602 01.43253   474   05 16 06.50    -04 55 57.4    .28-   .05-
1602 02.42748   474   05 13 20.40    -05 23 41.6    .14-   .30-
1602 02.43453   474   05 13 19.23    -05 23 52.7    .15+   .22+
1602 02.44157   474   05 13 18.03    -05 24 04.4    .04-   .12+
```

```
Orbital elements: 2016 BD39
  Perihelion 2016 May 8.973329 +/- 0.438 TT = 23:21:35 (JD 2457517.473329)
Epoch 2016 Feb 3.0 TT = JDT 2457421.5 Earth MOID: 0.3321 Ve: 0.0659
M 300.53252 +/- 0.43             Find_Orb
n  0.61962498 +/- 0.00716    Peri. 324.21992 +/- 0.15
a  1.36264721 +/- 0.0105     Node 277.52896 +/- 0.17
e  0.5459849 +/- 0.00402     Incl. 36.15706 +/- 0.9
P  1.59/580.99d       H 20.0  G 0.15  U 9.4
q 0.61866228 +/- 0.000754   Q 2.10663215 +/- 0.0216
From 17 observations 2016 Jan. 30-Feb. 3; mean residual 0".20

1601 30.32211   F51   05 22 15.728   -03 54 59.03   .18+   .11+
1601 30.34872   F51   05 22 10.775   -03 55 46.71   .10+   .06-
1601 30.36203   F51   05 22 08.290   -03 56 10.43   .11-   .04-
1602 01.06386   807   05 17 09.55    -04 45 32.7    .02+   .03+
1602 01.06667   807   05 17 09.05    -04 45 37.8    .02-   .27-
1602 01.06934   807   05 17 08.57    -04 45 42.3    .14-   .20-
1602 01.42478   474   05 16 07.88    -04 55 44.1    .07+   .10+
1602 01.42831   474   05 16 07.25    -04 55 50.1    .17-   .08+
1602 01.43253   474   05 16 06.50    -04 55 57.4    .41-   .08-
1602 02.169781  W85   05 14 02.57    -05 16 37.0    .04+   .23+
1602 02.175629  W85   05 14 01.56    -05 16 46.8    .23-   .11+
1602 02.181839  W85   05 14 00.53    -05 16 57.0    .10+   .20+
1602 02.42748   474   05 13 20.40    -05 23 41.6    .00    .37-
1602 02.43453   474   05 13 19.23    -05 23 52.7    .28+   .15+
1602 02.44157   474   05 13 18.03    -05 24 04.4    .08+   .05+
1602 02.64696   323   05 12 44.12    -05 29 44.4    .50+   .33+
1602 03.56465   323   05 10 16.78    -05 54 32.5    .27-   .36-
```

```
Orbital elements: 2016 BD39
  Perihelion 2016 May 8.108801 +/- 0.00105 TT = 2:36:40 (JD 2457516.608801)
Epoch 2016 Mar 14.0 TT = JDT 2457461.5 Earth MOID: 0.3287 Ve: 0.0643
M 325.32202 +/- 0.0037           Find_Orb
n  0.62926388 +/- 7.38e-5    Peri. 324.30968 +/- 0.0025
a  1.34869633 +/- 0.000105   Node 277.19170 +/- 0.00056
e  0.5398620 +/- 3.43e-5     Incl. 34.43560 +/- 0.0046
P  1.57/572.09d       H 20.2  G 0.15  U 6.4
q 0.62058633 +/- 5.57e-6   Q 2.07680632 +/- 0.000208
From 61 observations 2016 Jan. 30-Mar. 14; mean residual 0".47

1601 30.32211   F51   05 22 15.728   -03 54 59.03   .12+   .26+
1601 30.34872   F51   05 22 10.775   -03 55 46.71   .10+   .09+
1601 30.36203   F51   05 22 08.290   -03 56 10.43   .08-   .11+
1602 01.06386   807   05 17 09.55    -04 45 32.7    .18-   .24-
1602 01.06667   807   05 17 09.05    -04 45 37.8    .22-   .53-
1602 01.06934   807   05 17 08.57    -04 45 42.3    .33-   .47-
1602 01.42478   474   05 16 07.88    -04 55 44.1    .04-   .18-
1602 01.42831   474   05 16 07.25    -04 55 50.1    .28-   .20-
1602 01.43253   474   05 16 06.50    -04 55 57.4    .51-   .36-
1602 02.169781  W85   05 14 02.57    -05 16 37.0    .22+   .29+
1602 02.175629  W85   05 14 01.56    -05 16 46.8    .04-   .18+
1602 02.181839  W85   05 14 00.53    -05 16 57.0    .31+   .27+
1602 02.42748   474   05 13 20.40    -05 23 41.6    .06+   .27-
1602 02.43453   474   05 13 19.23    -05 23 52.7    .36+   .25+
1602 02.44157   474   05 13 18.03    -05 24 04.4    .18+   .16+
1602 02.64696   323   05 12 44.12    -05 29 44.4    .78+   .62+
1602 03.56465   323   05 10 16.78    -05 54 32.5    .11+   .53+
1602 04.14282   807   05 08 45.68    -06 09 51.1    .06+   .63+
```

Figure 10: Find_Orb data for P10rRRx before, with, and after my observations.
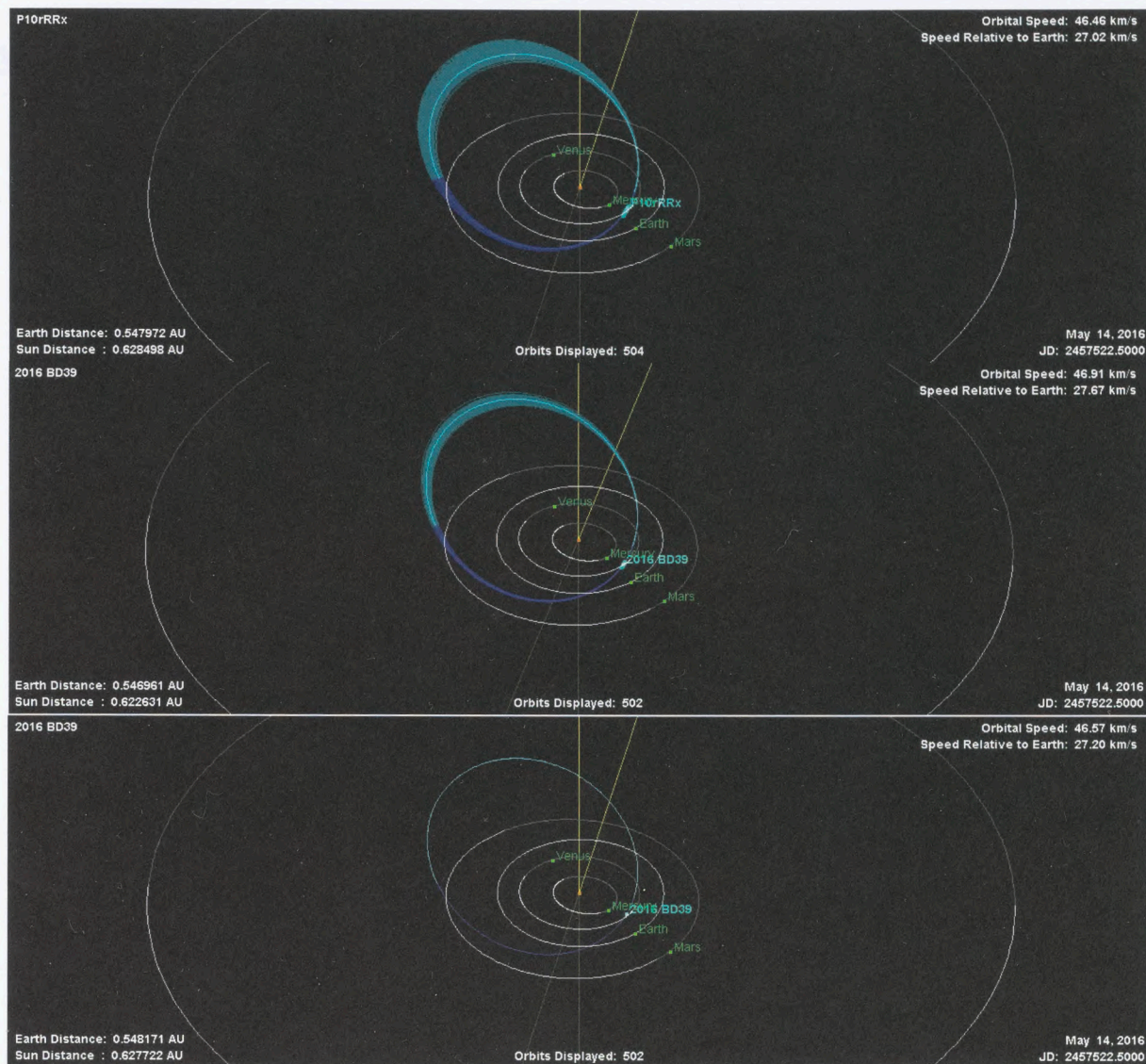
Figure 11: OrbitMaster visualizations for P10rRRx before, with, and after my observations

XC85137 (CL137)


```
Orbital elements: XC85137
  Perihelion 2015 Dec 23.997437 +/- 3.17 TT = 23:56:18 (JD 2457380.497437)
Epoch 2016 Feb  9.0 TT = JDT 2457427.5  Earth MOID: 0.0037  Ve: 0.0295
M 11.92286 +/- 7          Ma: 0.0430        Find_Orb
n  0.25366408 +/- 0.178      Peri.  249.60519 +/- 3.2
a  2.47151582 +/- 1.15       Node  153.38943 +/- 3.1
e  0.7869541 +/- 0.105       Incl.   0.73423 +/- 0.09
P  3.89          H 25.5  G 0.15  U 11.6
q 0.52654615 +/- 0.0342  Q 4.41648550 +/- 6.2
From 16 observations 2016 Feb. 9 (4.4 hr); mean residual 0".22
```

1602 09.25184	G96	09 16 57.33	+11 53 09.7	.06+	.11-
1602 09.25693	G96	09 16 56.18	+11 53 38.0	.07+	.02-
1602 09.26201	G96	09 16 55.04	+11 54 06.2	.20+	.14+
1602 09.26710	G96	09 16 53.89	+11 54 34.2	.21+	.15+
1602 09.28647	I52	09 16 49.51	+11 56 19.8	.10+	.27+
1602 09.29082	I52	09 16 48.52	+11 56 42.9	.06-	.09-
1602 09.29741	I52	09 16 47.02	+11 57 18.0	.34-	.39-
1602 09.30066	I52	09 16 46.29	+11 57 35.9	.36-	.12+
1602 09.36877	I52	09 16 31.40	+12 03 30.0	.26-	.10-
1602 09.37349	I52	09 16 30.42	+12 03 53.8	.03-	.16-
1602 09.37999	I52	09 16 29.06	+12 04 26.7	.02-	.03+
1602 09.38495	I52	09 16 28.05	+12 04 51.6	.27+	.07+
1602 09.42462	G96	09 16 20.09	+12 08 06.8	.23+	.16-
1602 09.42865	G96	09 16 19.29	+12 08 26.3	.10-	.19-
1602 09.43266	G96	09 16 18.54	+12 08 45.6	.16+	.27-
1602 09.43667	G96	09 16 17.76	+12 09 05.9	.11-	.71+

```
Orbital elements: XC85137
  Perihelion 2015 Dec 21.350209 +/- 0.111 TT = 8:24:18 (JD 2457377.850209)
Epoch 2016 Feb  9.0 TT = JDT 2457427.5  Earth MOID: 0.0036  Ve: 0.0278
M 18.55640 +/- 0.26        Ma: 0.0389        Find_Orb
n  0.37374591 +/- 0.00443     Peri.  251.35814 +/- 0.15
a  1.90876186 +/- 0.0151      Node  151.79243 +/- 0.16
e  0.7091391 +/- 0.00285      Incl.   0.77177 +/- 0.010
P  2.64/963.20d        H 25.8  G 0.15  U 9.1
q 0.55518417 +/- 0.00105  Q 3.26233955 +/- 0.0316
From 20 observations 2016 Feb. 9 (10.8 hr); mean residual 0".25
```

1602 09.26201	G96	09 16 55.04	+11 54 06.2	.19+	.13+
1602 09.26710	G96	09 16 53.89	+11 54 34.2	.18+	.15+
1602 09.28647	I52	09 16 49.51	+11 56 19.8	.05+	.27+
1602 09.29082	I52	09 16 48.52	+11 56 42.9	.10-	.10-
1602 09.29741	I52	09 16 47.02	+11 57 18.0	.38-	.39-
1602 09.30066	I52	09 16 46.29	+11 57 35.9	.39-	.12+
1602 09.36877	I52	09 16 31.40	+12 03 30.0	.11-	.09-
1602 09.37349	I52	09 16 30.42	+12 03 53.8	.12+	.15-
1602 09.37999	I52	09 16 29.06	+12 04 26.7	.13+	.04+
1602 09.38495	I52	09 16 28.05	+12 04 51.6	.42+	.09+
1602 09.42462	G96	09 16 20.09	+12 08 06.8	.16+	.13-
1602 09.42865	G96	09 16 19.29	+12 08 26.3	.21-	.16-
1602 09.43266	G96	09 16 18.54	+12 08 45.6	.00	.24-
1602 09.43667	G96	09 16 17.76	+12 09 05.9	.32-	.74+
1602 09.64242	323	09 15 59.81	+12 28 26.6	.23-	.64-
1602 09.65936	323	09 15 56.58	+12 29 42.7	.25+	.32+
1602 09.67168	323	09 15 54.21	+12 30 36.7	.18+	.29+
1602 09.70390	323	09 15 48.07	+12 32 55.2	.15-	.05-

```
Orbital elements: 2016 CL137
  Perihelion 2015 Dec 21.418325 +/- 0.0208 TT = 10:02:23 (JD 2457377.918325)
Epoch 2016 Feb 12.0 TT = JDT 2457430.5  Earth MOID: 0.0035  Ve: 0.0278
M 19.51733 +/- 0.057          Find_Orb
n  0.37118124 +/- 0.000946     Peri.  251.23125 +/- 0.0042
a  1.91754414 +/- 0.00326      Node  151.92942 +/- 0.0048
e  0.7107790 +/- 0.000609      Incl.   0.76267 +/- 0.0008
P  2.66/969.86d        H 25.9  G 0.15  U 8.1
q 0.55459385 +/- 0.000226  Q 3.28049442 +/- 0.00676
From 44 observations 2016 Feb. 9-12; mean residual 0".32
```

1602 09.25184	G96	09 16 57.33	+11 53 09.7	.13+	.10-
1602 09.25693	G96	09 16 56.18	+11 53 38.0	.12+	.01-
1602 09.26201	G96	09 16 55.04	+11 54 06.2	.23+	.15+
1602 09.26710	G96	09 16 53.89	+11 54 34.2	.23+	.16+
1602 09.28647	I52	09 16 49.51	+11 56 19.8	.12+	.28+
1602 09.29082	I52	09 16 48.52	+11 56 42.9	.03-	.09-
1602 09.29741	I52	09 16 47.02	+11 57 18.0	.30-	.39-
1602 09.30066	I52	09 16 46.29	+11 57 35.9	.31-	.12+
1602 09.36877	I52	09 16 31.40	+12 03 30.0	.01+	.08-
1602 09.37349	I52	09 16 30.42	+12 03 53.8	.24+	.14-
1602 09.37999	I52	09 16 29.06	+12 04 26.7	.25+	.05+
1602 09.38495	I52	09 16 28.05	+12 04 51.6	.55+	.10+
1602 09.42462	G96	09 16 20.09	+12 08 06.8	.29+	.09-
1602 09.42865	G96	09 16 19.29	+12 08 26.3	.08-	.12-
1602 09.43266	G96	09 16 18.54	+12 08 45.6	.13+	.19-
1602 09.43667	G96	09 16 17.76	+12 09 05.9	.19-	.79+
1602 09.64242	323	09 15 59.81	+12 28 26.6	.37-	.36-
1602 09.65900	323	09 15 56.65	+12 29 40.5	.11+	.03+

Figure 12: Find_Orb data for XC85137 before, with, and after my observations
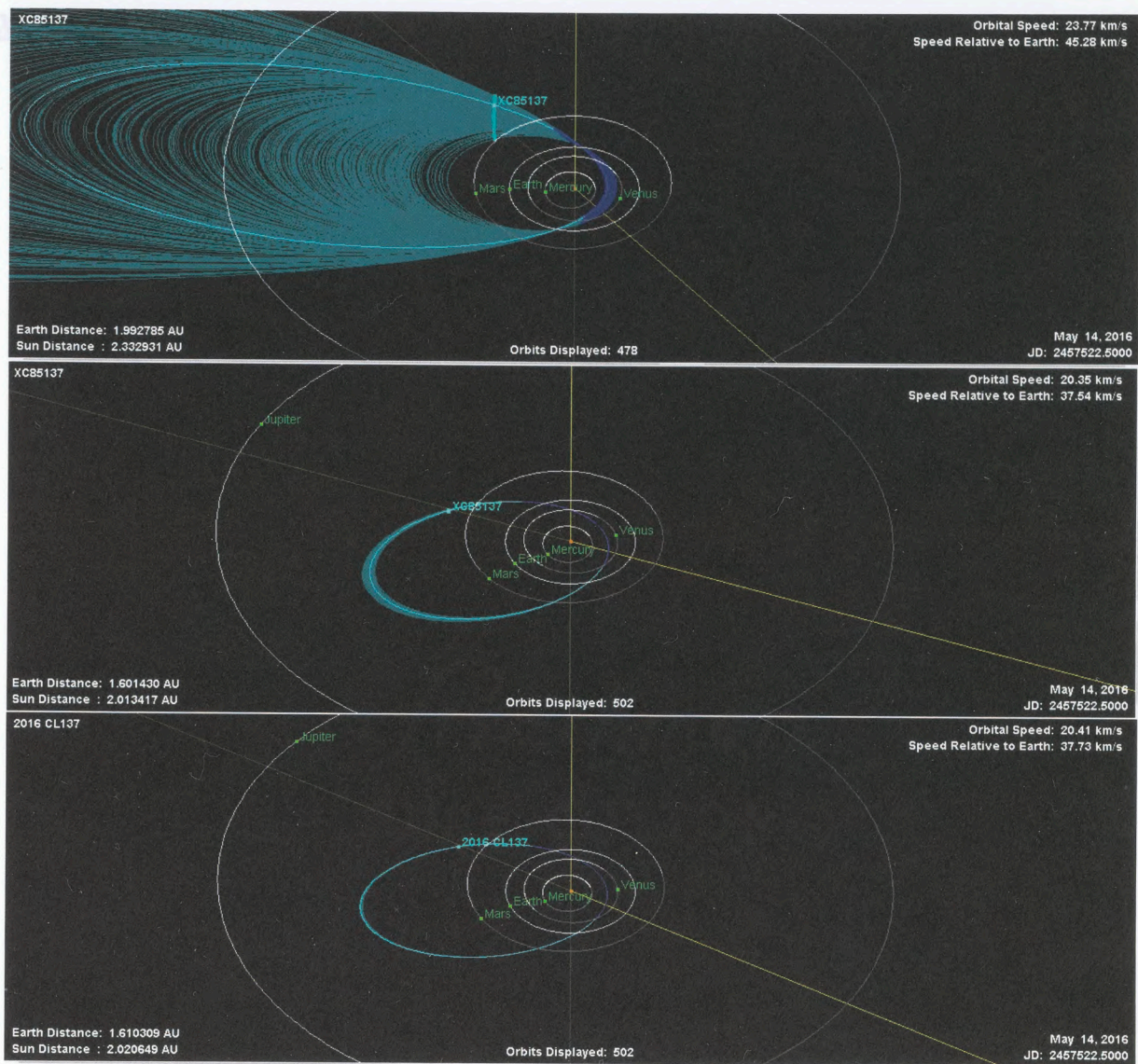
Figure 13: OrbitMaster visualizations for XC85137 before, with, and after my observations

XC83AD6 (2016 CD137)

Orbital elements: 2016 CD137
  Perihelion 2016 Apr 24.325202 +/- 0.039 TT = 7:48:17 (JD 2457502.825202)
Epoch 2016 Feb 9.0 TT = JDT 2457427.5 Earth MOID: 0.0022 Find_Orb
M 294.03706 +/- 0.049
 n 0.87570864 +/- 0.00023   Peri. 94.08260 +/- 0.027
 a 1.08200588 +/- 0.00019   Node 138.16131 +/- 0.0009
 e 0.2327492 +/- 0.000646   Incl.   4.64354 +/- 0.008
 P 1.13/411.09d   H 26.1 G 0.15 U 7.1
 q 0.83016981 +/- 0.000581   Q 1.33384195 +/- 0.000905
From 31 observations 2016 Feb. 8-9 (25.3 hr); mean residual 0".26

1602 08.42566	I52	09 49 48.25	+14 51 37.7	.20+	.62+
1602 08.42987	I52	09 49 48.25	+14 52 02.1	.10-	.17-
1602 08.430707	H01	09 49 47.84	+14 52 01.5	.22-	.04-
1602 08.56982	474	09 50 01.40	+15 09 58.3	.18-	.25-
1602 08.57218	474	09 50 01.41	+15 10 13.3	.21-	.02-
1602 08.57453	474	09 50 01.45	+15 10 28.2	.19+	.18+
1602 08.57689	474	09 50 01.47	+15 10 42.8	.30+	.03+
1602 09.26883	I52	09 50 51.44	+16 24 02.9	.24-	.04+
1602 09.27024	I52	09 50 51.45	+16 24 13.4	.19-	.42+
1602 09.27165	I52	09 50 51.48	+16 24 22.7	.16+	.40-
1602 09.27351	I52	09 50 51.46	+16 24 36.3	.24-	.14-
1602 09.32112	I52	09 50 51.50	+16 30 17.9	.29-	.37+
1602 09.32437	I52	09 50 51.51	+16 30 40.9	.11-	.12+
1602 09.32579	I52	09 50 51.52	+16 30 51.3	.06+	.37+
1602 09.32991	I52	09 50 51.51	+16 31 20.5	.02-	.11+
1602 09.39493	926	09 50 51.56	+16 39 07.5	.60+	.30+
1602 09.39991	926	09 50 51.55	+16 39 42.6	.18+	.03-
1602 09.40491	926	09 50 51.53	+16 40 17.6	.44-	.58-

Orbital elements: 2016 CD137
  Perihelion 2016 Apr 24.289061 +/- 0.0197 TT = 6:56:14 (JD 2457502.789061)
Epoch 2016 Feb 9.0 TT = JDT 2457427.5 Earth MOID: 0.0023 Find_Orb
M 294.07631 +/- 0.032
 n 0.87560771 +/- 0.000214   Peri. 94.11312 +/- 0.007
 a 1.08208903 +/- 0.000177   Node 138.16032 +/- 0.00032
 e 0.2333442 +/- 0.000347   Incl.   4.63486 +/- 0.0042
 P 1.13/411.14d   H 26.2 G 0.15 U 7.1
 q 0.82958976 +/- 0.000247   Q 1.33458830 +/- 0.000588
From 34 observations 2016 Feb. 8-9 (33.3 hr); mean residual 0".29

1602 08.56982	474	09 50 01.40	+15 09 58.3	.18-	.25-
1602 08.57218	474	09 50 01.41	+15 10 13.3	.21-	.01-
1602 08.57453	474	09 50 01.45	+15 10 28.2	.20+	.19+
1602 08.57689	474	09 50 01.47	+15 10 42.8	.31+	.03+
1602 09.26883	I52	09 50 51.44	+16 24 02.9	.22-	.17+
1602 09.27024	I52	09 50 51.45	+16 24 13.4	.17-	.55+
1602 09.27165	I52	09 50 51.48	+16 24 22.7	.18+	.27-
1602 09.27351	I52	09 50 51.46	+16 24 36.3	.21-	.02-
1602 09.32112	I52	09 50 51.50	+16 30 17.9	.20-	.38+
1602 09.32437	I52	09 50 51.51	+16 30 40.9	.00	.13+
1602 09.32579	I52	09 50 51.52	+16 30 51.3	.16+	.37+
1602 09.32991	I52	09 50 51.51	+16 31 20.5	.09+	.11+
1602 09.39493	926	09 50 51.56	+16 39 07.5	.81+	.14+
1602 09.39991	926	09 50 51.55	+16 39 42.6	.40+	.20-
1602 09.40491	926	09 50 51.53	+16 40 17.6	.22-	.77-
1602 09.68583	323	09 51 17.75	+17 18 25.3	.41-	.46+
1602 09.71918	323	09 51 17.76	+17 22 40.1	.68-	.06-
1602 09.74076	323	09 51 17.88	+17 25 24.9	.45+	.14-

Orbital elements: 2016 CD137
  Perihelion 2016 Apr 24.249567 +/- 0.00357 TT = 5:59:22 (JD 2457502.749567)
Epoch 2016 Feb 18.0 TT = JDT 2457436.5 Earth MOID: 0.0024 Find_Orb
M 302.00781 +/- 0.006
 n 0.87535941 +/- 5.33e-5   Peri. 94.13671 +/- 0.00036
 a 1.08229365 +/- 4.39e-5   Node 138.12976 +/- 0.00011
 e 0.2337611 +/- 6.65e-5   Incl.   4.60982 +/- 0.0013
 P 1.13/411.25d   H 26.1 G 0.15 U 6.1
 q 0.82929539 +/- 3.84e-5   Q 1.33529191 +/- 0.000126
From 108 observations 2016 Feb. 8-18; mean residual 0".46

1602 08.35161	G96	09 49 48.37	+14 44 13.2	.19+	.13-
1602 08.35675	G96	09 49 48.35	+14 44 44.2	.30+	.01-
1602 08.36189	G96	09 49 48.31	+14 45 14.9	.10+	.18-
1602 08.36704	G96	09 49 48.28	+14 45 45.9	.02+	.09-
1602 08.39456	G96	09 49 48.19	+14 48 30.8	.01-	.21-
1602 08.40059	G96	09 49 48.21	+14 49 07.0	.36+	.12-
1602 08.403118	H01	09 49 47.66	+14 49 16.8	.49-	.02-
1602 08.40663	G96	09 49 48.19	+14 49 43.0	.08+	.28-
1602 08.41266	G96	09 49 48.21	+14 50 19.3	.28+	.07-
1602 08.413888	H01	09 49 47.73	+14 50 21.1	.05-	.05-
1602 08.41978	I52	09 49 48.22	+14 51 01.3	.19+	.67-
1602 08.42422	I52	09 49 48.22	+14 51 28.0	.04-	.52-
1602 08.424845	H01	09 49 47.80	+14 51 26.5	.02+	.07-
1602 08.42566	I52	09 49 48.25	+14 51 37.7	.31+	.57+
1602 08.42987	I52	09 49 48.25	+14 52 02.1	.02+	.20-
1602 08.430707	H01	09 49 47.84	+14 52 01.5	.08-	.06-
1602 08.56982	474	09 50 01.40	+15 09 58.3	.16-	.59-
1602 08.57218	474	09 50 01.41	+15 10 13.3	.18-	.34-

Figure 14: Find_Orb data for XC83AD6 before, with, and after my observations
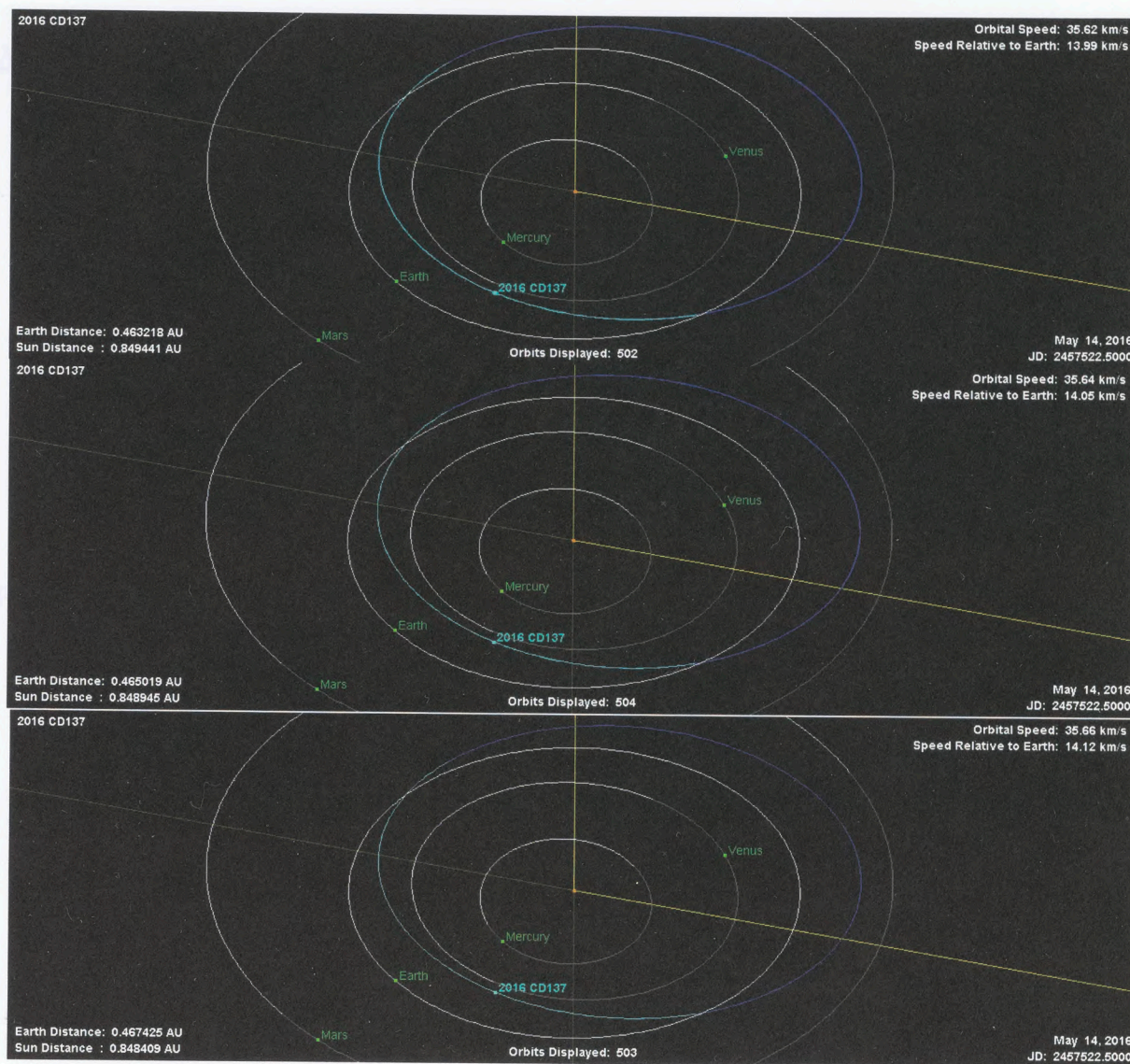
Figure 15: OrbitMaster visualizations for XC83AD6 before, with, and after my observations

XC20069 (2002 TT₂₀₆)

Figure 16: Find_Orb data for XC20069 with and after my observations. There is no before period because Find_Orb could not generate a reasonable orbit given such little data.

Figure 17: OrbitMaster visualizations for before, during, and after my observations. Due to the inability of Find_Orb to give reasonable orbits for the "during" phase adding only my observations, the "during" phase shown here includes subsequent observations from Haute Provence.

Figure 17: OrbitMaster visualizations for before, during, and after my observations. Due to the inability of Find_Orb to give reasonable orbits for the "during" phase adding only my observations, the "during" phase shown here includes subsequent observations from Haute Provence.

XC1EF0C (2016 CH$_{137}$)

Orbital elements: 2016 CH137
Perihelion 2015 Dec 26.480107 +/- 0.0221 TT = 11:31:21 (JD 2457382.980107
Epoch 2016 Feb 10.0 TT = JDT 2457428.5   Earth MOID: 0.0060   Ve: 0.0146
M 12.29419 +/- 0.056   Find_Orb
n 0.27008393 +/- 0.00111   Peri. 74.94905 +/- 0.0012
a 2.37030124 +/- 0.00651   Node 320.63733 +/- 0.00032
e 0.8108287 +/- 0.000617   Incl.   8.23758 +/- 0.007
P 3.65   H 25.8 G 0.15 U 8.2
q 0.44839283 +/- 0.00023   Q 4.29220964 +/- 0.0132
From 42 observations 2016 Feb. 9-10 (24.1 hr); mean residual 0".29

1602 09.30723	703	08 58 06.81	+24 35 32.3	.21-	.83-
1602 09.32295	703	08 57 55.52	+24 26 19.5	.04-	.08-
1602 09.33160	703	08 57 49.42	+24 21 18.3	.10-	.83-
1602 09.36351	703	08 57 27.76	+24 03 15.4	.34+	.12-
1602 09.37263	703	08 57 21.78	+23 58 13.0	.07+	.18+
1602 09.37399	I52	08 57 20.93	+23 57 27.9	.17+	.06+
1602 09.38049	I52	08 57 16.77	+23 53 54.8	.30+	.52+
1602 09.38175	703	08 57 15.92	+23 53 13.3	.06-	.15+
1602 09.38545	I52	08 57 13.61	+23 51 12.6	.07+	.25+
1602 09.40020	703	08 57 04.42	+23 43 16.1	.18-	.02+
1602 09.40939	703	08 56 58.93	+23 38 23.2	.64+	.01+
1602 09.415895	H01	08 56 54.34	+23 34 43.3	.11-	.02-
1602 09.422458	H01	08 56 50.56	+23 31 17.3	.16-	.07-
1602 09.42775	703	08 56 48.13	+23 28 46.3	.27-	.57-
1602 09.429231	H01	08 56 46.73	+23 27 46.3	.12-	.10-
1602 09.43413	I52	08 56 44.54	+23 25 29.4	.12-	.14+
1602 09.436367	H01	08 56 42.75	+23 24 05.7	.29-	.15-
1602 09.43676	I52	08 56 43.08	+23 24 08.5	.09+	.26+

Orbital elements: 2016 CH137
Perihelion 2015 Dec 26.470298 +/- 0.0173 TT = 11:17:13 (JD 2457382.970298
Epoch 2016 Feb 10.0 TT = JDT 2457428.5   Earth MOID: 0.0060   Ve: 0.0146
M 12.31891 +/- 0.044   Find_Orb
n 0.27056881 +/- 0.000877   Peri. 74.94964 +/- 0.0009
a 2.36746859 +/- 0.00511   Node 320.63743 +/- 0.00027
e 0.8105577 +/- 0.000485   Incl.   8.23511 +/- 0.006
P 3.64   H 25.9 G 0.15 U 8.0
q 0.44849855 +/- 0.00018   Q 4.28643864 +/- 0.0104
From 45 observations 2016 Feb. 9-10 (26.5 hr); mean residual 0".28

1602 10.117129	H01	08 53 26.18	+19 20 47.7	.12-	.27-
1602 10.122294	H01	08 53 24.72	+19 19 31.2	.06-	.35-
1602 10.19353	I52	08 53 04.94	+19 02 29.9	.06-	.01-
1602 10.19721	I52	08 53 03.86	+19 01 38.4	.09-	.03+
1602 10.20073	I52	08 53 02.82	+19 00 49.4	.22-	.20+
1602 10.20252	I52	08 53 02.29	+19 00 23.9	.30-	.34-
1602 10.23414	926	08 52 53.14	+18 53 12.0	.43+	.03+
1602 10.23664	926	08 52 52.39	+18 52 37.6	.21+	.26-
1602 10.23910	926	08 52 51.62	+18 52 04.6	.47-	.25+
1602 10.26453	926	08 52 44.21	+18 46 21.2	.20-	.26+
1602 10.26671	926	08 52 43.59	+18 45 51.6	.02-	.16-
1602 10.26926	926	08 52 42.85	+18 45 17.7	.03-	.04+
1602 10.30826	926	08 52 31.72	+18 36 42.9	.01-	.08+
1602 10.31072	926	08 52 31.05	+18 36 11.3	.26+	.55+
1602 10.31315	926	08 52 30.40	+18 35 39.7	.66+	.58+
1602 10.39741	G52	08 52 11.05	+18 17 32.4	.02-	.03+
1602 10.40404	G52	08 52 09.42	+18 16 11.0	.08-	.19-
1602 10.41082	G52	08 52 07.78	+18 14 48.4	.03-	.11-

Orbital elements: 2016 CH137
Perihelion 2015 Dec 26.470590 +/- 0.0128 TT = 11:17:39 (JD 2457382.970590
Epoch 2016 Feb 13.0 TT = JDT 2457431.5   Earth MOID: 0.0060   Ve: 0.0146
M 13.13084 +/- 0.035   Find_Orb
n 0.27057500 +/- 0.000652   Peri. 74.94832 +/- 0.00020
a 2.36743246 +/- 0.0038   Node 320.63749 +/- 0.00020
e 0.8105599 +/- 0.00036   Incl.   8.23315 +/- 0.0047
P 3.64   H 25.9 G 0.15 U 7.8
q 0.44848641 +/- 0.000132   Q 4.28637850 +/- 0.00771
From 71 observations 2016 Feb. 9-13; mean residual 0".33

1602 10.30826	926	08 52 31.72	+18 36 42.9	.00	.00
1602 10.31072	926	08 52 31.05	+18 36 11.3	.27+	.47+
1602 10.31315	926	08 52 30.40	+18 35 39.7	.67+	.49+
1602 10.39741	G52	08 52 11.05	+18 17 32.4	.03-	.17-
1602 10.40404	G52	08 52 09.42	+18 16 11.0	.08-	.40-
1602 10.41082	G52	08 52 07.78	+18 14 48.4	.04-	.33-
1602 10.48566	474	08 52 03.00	+18 04 50.3	.89+	.27-
1602 10.48686	474	08 52 02.67	+18 04 36.6	.22+	.32-
1602 10.48806	474	08 52 02.40	+18 04 23.2	.41+	.07-
1602 10.48925	474	08 52 02.06	+18 04 09.0	.44-	.75-
1602 10.57542	E23	08 51 45.81	+17 47 57.9	.61-	.19+
1602 10.59729	E23	08 51 40.89	+17 44 06.0	.89+	1.4+
1602 10.92174	C77	08 51 01.55	+16 49 16.7	.38-	.26+
1602 10.92805	C77	08 51 00.45	+16 48 24.3	.02+	.28+
1602 10.93456	C77	08 50 59.26	+16 47 29.7	.39-	.40-
1602 11.15006	204	08 50 25.90	+16 19 09.3	.17+	.03+
1602 11.16059	204	08 50 24.64	+16 17 50.7	.23-	.25-
1602 11.21537	926	08 50 31.53	+16 12 22.4	.30-	.20+

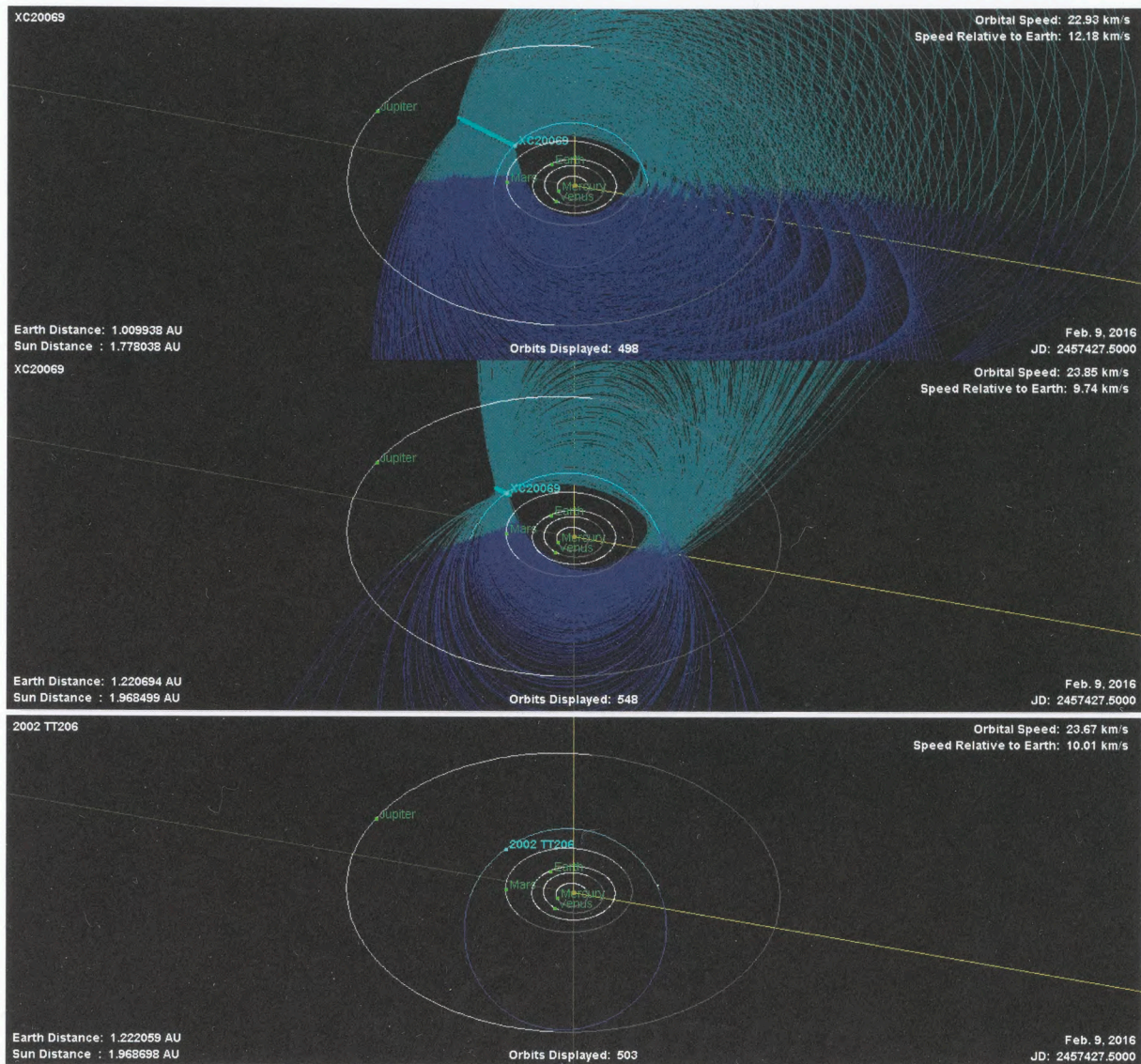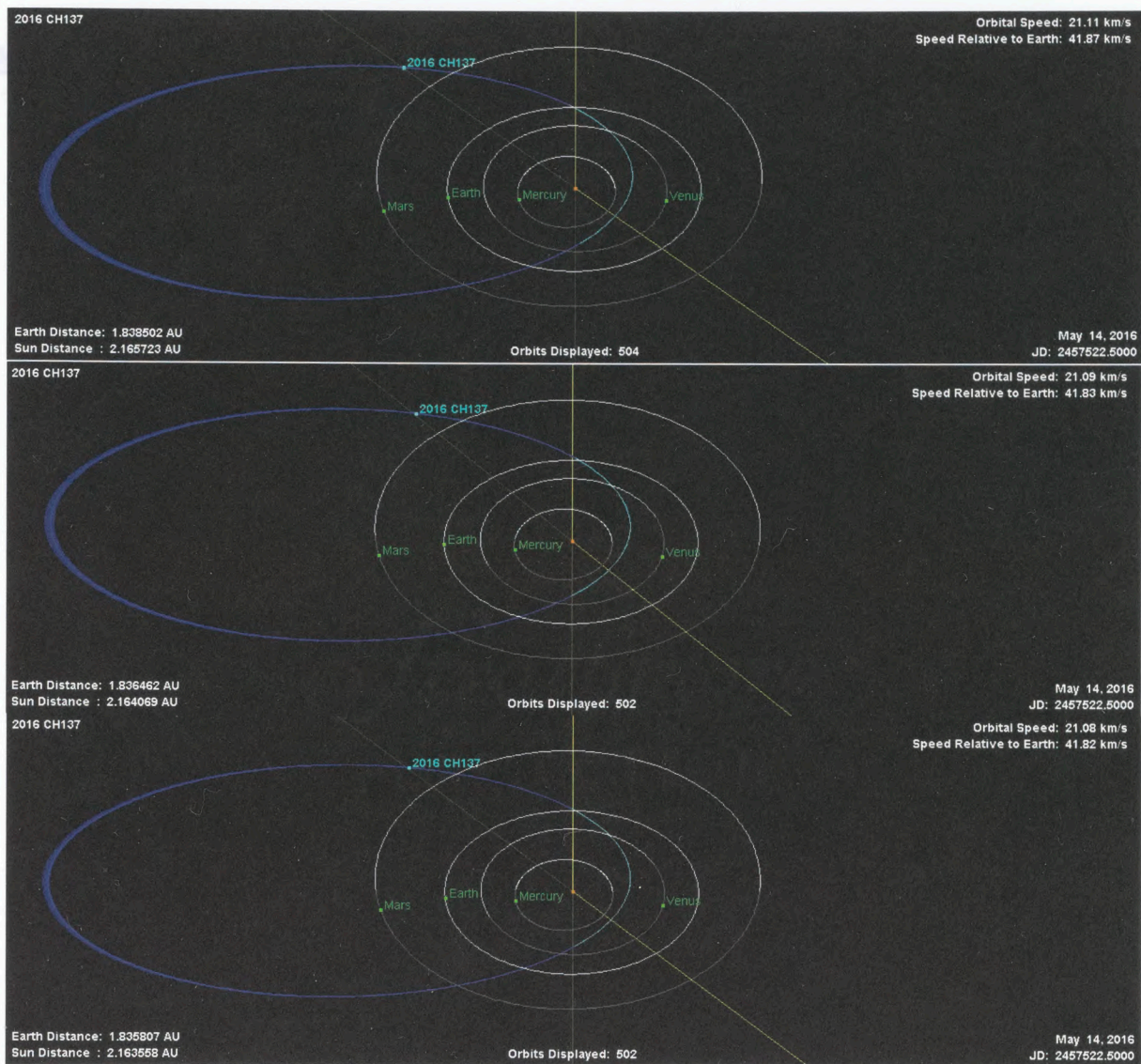Figure 18: Find_Orb data for XC1EF0C before, with, and after my observations

Figure 19: OrbitMaster visualizations for XC1EF0C before, with, and after my observations

Figure 20: Find_Orb data for XC22469 before, with, and after my observations

XC22469 (2016 CM₁₉₄)

Orbital elements: 2016 CM194
Perihelion 2016 Mar 27.880802 +/- 0.0449 TT = 21:08:21 (JD 2457475.380802
Epoch 2016 Feb 12.0 TT = JDT 2457430.5   Earth MOID: 0.0003 Ma: 0.0030
M 335.14265 +/- 0.10   Find_Orb
n 0.55385244 +/- 0.00188   Peri. 239.43143 +/- 0.007
a 1.46849789 +/- 0.00332   Node   323.67124 +/- 0.0022
e 0.4260246 +/- 0.00152   Incl.   8.29385 +/- 0.020
P 1.78/649.98d   H 27.4 G 0.15 U 8.5
q 0.84288156 +/- 0.000331   Q 2.09411423 +/- 0.007
From 36 observations 2016 Feb. 12 (3.8 hr); mean residual 0".42

1602 12.22173	703	09 02 32.07	+39 41 57.6	.28-	.31+
1602 12.22634	703	09 02 24.83	+39 41 43.9	.22-	.15-
1602 12.23095	703	09 02 17.58	+39 41 29.9	.76+	.27-
1602 12.23559	703	09 02 10.01	+39 41 15.8	.37-	.27+
1602 12.29965	703	09 00 18.29	+39 36 37.9	.07-	.28+
1602 12.30668	703	09 00 05.22	+39 35 58.0	.90+	.30+
1602 12.31365	703	08 59 51.93	+39 35 16.0	.19-	.13-
1602 12.32046	703	08 59 38.90	+39 34 33.0	.11-	.57-
1602 12.34200	F51	09 00 16.749	+39 35 47.52	.03-	.05+
1602 12.34921	703	08 58 42.38	+39 31 12.3	.51-	.19+
1602 12.35040	I52	08 58 40.11	+39 31 02.7	.32-	.01+
1602 12.35069	703	08 58 39.44	+39 31 00.1	.20-	.66-
1602 12.35089	H06	08 58 31.32	+39 30 21.0	1.1+	.64+
1602 12.35169	H06	08 58 29.57	+39 30 13.6	.75-	.25-
1602 12.35218	703	08 58 36.47	+39 30 49.9	.05+	.66+
1602 12.35249	H06	08 58 28.02	+39 30 06.7	.27-	.62-
1602 12.353093	H01	08 58 29.88	+39 29 47.8	.22-	.05-
1602 12.35329	H06	08 58 26.47	+39 30 00.2	.22+	.55-

Orbital elements: 2016 CM194
Perihelion 2016 Mar 27.894126 +/- 0.0294 TT = 21:27:32 (JD 2457475.394126
Epoch 2016 Feb 12.0 TT = JDT 2457430.5   Earth MOID: 0.0003 Ma: 0.0032
M 335.10934 +/- 0.07   Find_Orb
n 0.55443011 +/- 0.00122   Peri. 239.43282 +/- 0.0056
a 1.46747768 +/- 0.00216   Node   323.67189 +/- 0.0014
e 0.4255526 +/- 0.00099   Incl.   8.28748 +/- 0.013
P 1.78/649.30d   H 27.6 G 0.15 U 8.2
q 0.84298860 +/- 0.000214   Q 2.09196676 +/- 0.00454
From 45 observations 2016 Feb. 12 (4.2 hr); mean residual 0".39

1602 12.36747	H06	08 57 58.03	+39 27 59.8	.17+	.14+
1602 12.36880	H06	08 57 55.32	+39 27 48.2	.11-	.35+
1602 12.369854	H01	08 57 56.25	+39 27 25.9	.11-	.20-
1602 12.36994	G96	08 58 00.53	+39 28 24.3	.25+	.31+
1602 12.37012	H06	08 57 52.70	+39 27 36.2	.46+	.15+
1602 12.37145	H06	08 57 49.98	+39 27 24.3	.14+	.21+
1602 12.374638	H01	08 57 46.54	+39 26 43.3	.21-	.07-
1602 12.37553	G96	08 57 49.00	+39 27 35.7	.21-	.27+
1602 12.38114	G96	08 57 37.39	+39 26 45.4	.39-	.14+
1602 12.38366	G52	08 57 53.18	+39 25 18.1	.21+	.34-
1602 12.38550	G52	08 57 49.35	+39 25 03.0	.18+	.15-
1602 12.38674	G96	08 57 25.80	+39 25 54.1	.12+	.36+
1602 12.38734	G52	08 57 45.50	+39 24 47.4	.03+	.32-
1602 12.387633	H01	08 57 20.00	+39 24 42.0	.04-	.15-
1602 12.38919	G52	08 57 41.61	+39 24 31.7	.23-	.35-
1602 12.39104	G52	08 57 37.77	+39 24 15.9	.19+	.32-
1602 12.39289	G52	08 57 33.86	+39 24 00.2	.10-	.03-
1602 12.39473	G52	08 57 30.02	+39 23 44.3	.29+	.13+

Orbital elements: 2016 CM194
Perigee 2016 Feb 13.325177 +/- 5.74e-6 TT = 7:48:15 (JD 2457431.825177)
Epoch 2016 Feb 13.0 TT = JDT 2457431.5   Find_Orb
q 77343.6463 +/- 6.07   (J2000 equatorial)
H 27.8 G 0.15   Peri. 200.60429 +/- 0.00041
                            Node 255.45390 +/- 0.00008
e 26.9588686 +/- 0.00578   Incl. 136.24090 +/- 0.00010
From 117 observations 2016 Feb. 12-13 (23.2 hr); mean residual 0".76

1602 12.22173	703	09 02 32.07	+39 41 57.6	.19-	.01+
1602 12.22634	703	09 02 24.83	+39 41 43.9	.14-	.44-
1602 12.23095	703	09 02 17.58	+39 41 29.9	.83+	.55-
1602 12.23559	703	09 02 10.01	+39 41 15.8	.30-	.01-
1602 12.29965	703	09 00 18.29	+39 36 37.9	.04-	.14+
1602 12.30668	703	09 00 05.22	+39 35 58.0	.92+	.18+
1602 12.31365	703	08 59 51.93	+39 35 16.0	.17-	.23-
1602 12.32046	703	08 59 38.90	+39 34 33.0	.09-	.66-
1602 12.34200	F51	09 00 16.749	+39 35 47.52	.30-	.03-
1602 12.34921	703	08 58 42.38	+39 31 12.3	.53-	.19+
1602 12.35040	I52	08 58 40.11	+39 31 02.7	.34-	.01+
1602 12.35069	703	08 58 39.44	+39 31 00.1	.22-	.66-
1602 12.35089	H06	08 58 31.32	+39 30 21.0	1.1+	.65+
1602 12.35169	H06	08 58 29.57	+39 30 13.6	.75-	.24-
1602 12.35218	703	08 58 36.47	+39 30 49.9	.03+	.67+
1602 12.35249	H06	08 58 28.02	+39 30 06.7	.27-	.60-
1602 12.353093	H01	08 58 29.88	+39 29 47.8	.23-	.02-
1602 12.35329	H06	08 58 26.47	+39 30 00.2	.22+	.53-
1602 12.35347	F51	08 59 54.184	+39 35 07.04	.29-	.16-
1602 12.35366	703	08 58 33.54	+39 30 38.1	.57+	.41+

Figure 20: Find_Orb data for XC22469 before, with, and after my observations
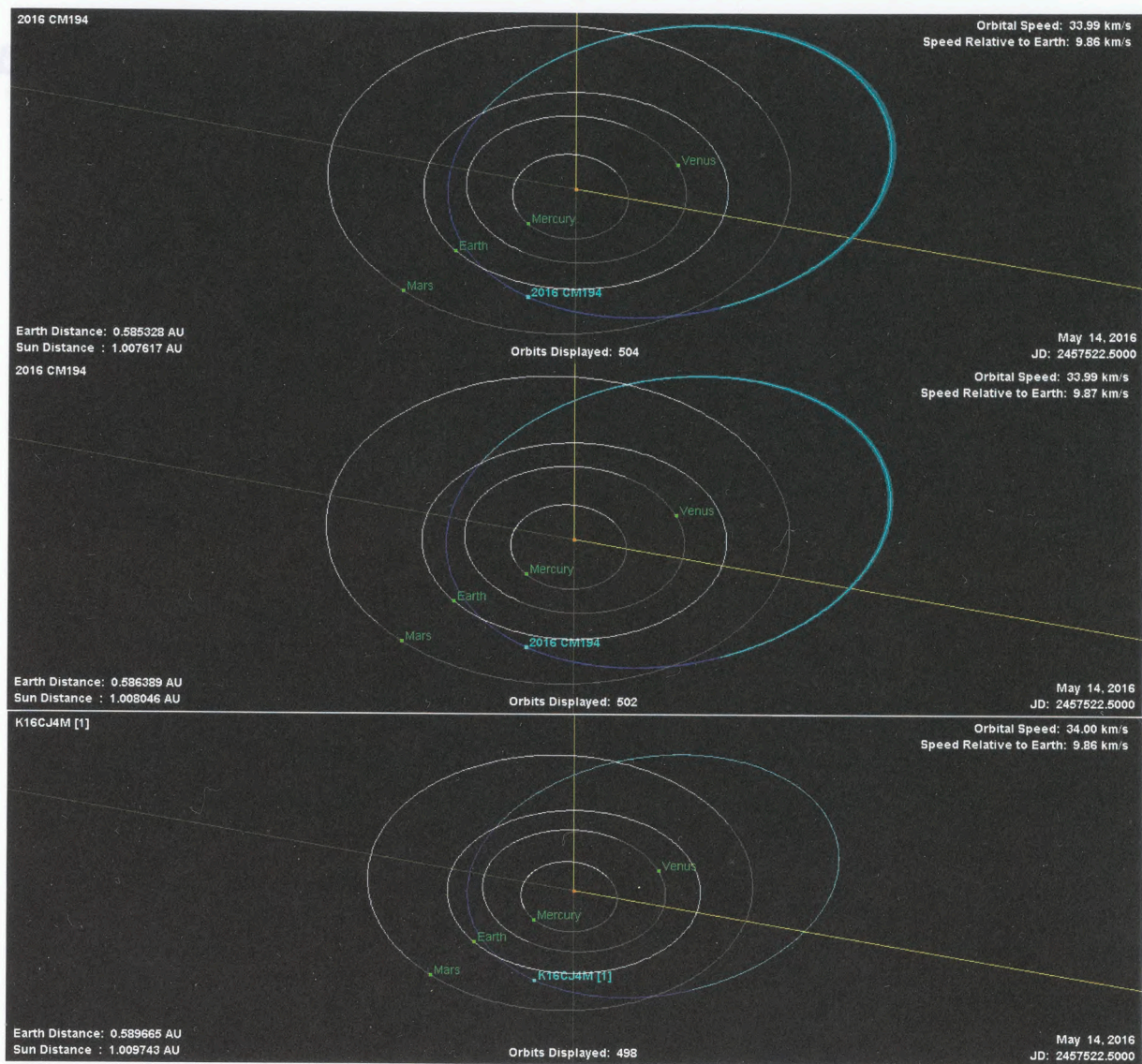
Figure 21: OrbitMaster visualizations for XC22469 before, with, and after my observations

P10sJtm (2016 CO$_{264}$)

Orbital elements: 2016 CO264
Perihelion 2016 Aug 15.248820 +/- 0.105 TT = 5:58:18 (JD 2457615.748820)
Epoch 2016 Feb 17.0 TT = JDT 2457435.5 Sa: 0.3045   Find_Orb
M 359.47041 +/- 0.015
n 0.00293807 +/- 8.61e-5   Peri. 66.68772 +/- 0.017
a 48.2792479 +/- 0.943   Node 178.10796 +/- 0.0040
e 0.9375068 +/- 0.00121   Incl. 129.84765 +/- 0.0051
P 335.46   H 16.1 G 0.15 U 6.5
q 3.01711997 +/- 0.000403   Q 93.5413759 +/- 1.97
From 28 observations 2016 Jan. 8-Feb. 17; mean residual 0".26

1602 04.49426	F51	12 16 04.78	+21 12 32.8	.25-	.13-
1602 04.50808	F51	12 16 03.88	+21 12 54.4	.15-	.09-
1602 04.52186	F51	12 16 02.99	+21 13 16.2	.07+	.21+
1602 14.44094	F51	12 03 29.862	+25 42 34.35	.21+	.31-
1602 14.45270	F51	12 03 28.799	+25 42 54.56	.03-	.03+
1602 14.46446	F51	12 03 27.771	+25 43 14.54	.21+	.14+
1602 15.33470	291	12 02 10.60	+26 07 43.5	.54+	.12+
1602 15.33798	291	12 02 10.27	+26 07 49.3	.11+	.35+
1602 15.34127	291	12 02 10.00	+26 07 54.6	.51+	.08+
1602 15.498759	568	12 01 55.749	+26 12 21.78	.11-	.09-
1602 15.500026	568	12 01 55.631	+26 12 23.94	.13-	.08-
1602 15.501295	568	12 01 55.516	+26 12 26.11	.12-	.06-
1602 16.52969	691	12 00 21.40	+26 41 29.6	.25+	.07+
1602 16.53496	691	12 00 20.93	+26 41 38.5	.55+	.05+
1602 16.54022	691	12 00 20.31	+26 41 47.5	1.2-	.14+
1602 17.322086	705	11 59 07.51	+27 03 57.6	.07-	.23-
1602 17.323109	705	11 59 07.40	+27 03 59.6	.23-	.02+
1602 17.324124	705	11 59 07.30	+27 04 01.1	.27-	.21-

Orbital elements: 2016 CO264
Perihelion 2016 Aug 15.239493 +/- 0.0987 TT = 5:44:52 (JD 2457615.739493)
Epoch 2016 Feb 17.0 TT = JDT 2457435.5 Sa: 0.3057   Find_Orb
M 359.47120 +/- 0.014
n 0.00293384 +/- 8.11e-5   Peri. 66.68535 +/- 0.016
a 48.3256505 +/- 0.89   Node 178.10814 +/- 0.0038
e 0.9375656 +/- 0.00114   Incl. 129.84777 +/- 0.0049
P 335.94   H 16.2 G 0.15 U 6.4
q 3.01717984 +/- 0.000382   Q 93.6341211 +/- 1.86
From 31 observations 2016 Jan. 8-Feb. 17; mean residual 0".25

1602 14.44094	F51	12 03 29.862	+25 42 34.35	.19+	.30-
1602 14.45270	F51	12 03 28.799	+25 42 54.56	.05-	.04+
1602 14.46446	F51	12 03 27.771	+25 43 14.54	.19+	.15+
1602 15.33470	291	12 02 10.60	+26 07 43.5	.51+	.13+
1602 15.33798	291	12 02 10.27	+26 07 49.3	.09+	.37+
1602 15.34127	291	12 02 10.00	+26 07 54.6	.48+	.09+
1602 15.498759	568	12 01 55.749	+26 12 21.78	.13-	.08-
1602 15.500026	568	12 01 55.631	+26 12 23.94	.16-	.06-
1602 15.501295	568	12 01 55.516	+26 12 26.11	.14-	.04-
1602 16.52969	691	12 00 21.40	+26 41 29.6	.21+	.09+
1602 16.53496	691	12 00 20.93	+26 41 38.5	.52+	.07+
1602 16.54022	691	12 00 20.31	+26 41 47.5	1.2-	.16+
1602 17.322086	705	11 59 07.51	+27 03 57.6	.10-	.21-
1602 17.323109	705	11 59 07.40	+27 03 59.6	.27-	.04+
1602 17.324124	705	11 59 07.30	+27 04 01.1	.30-	.19-
1602 17.42868	754	11 58 57.26	+27 06 58.6	.13+	.14-
1602 17.44159	754	11 58 56.02	+27 07 20.6	.07+	.08-
1602 17.45213	754	11 58 55.02	+27 07 38.6	.18+	.01+

Orbital elements: 2016 CO264
Perihelion 2016 Aug 15.294662 +/- 0.0584 TT = 7:04:18 (JD 2457615.794662)
Epoch 2016 Feb 26.0 TT = JDT 2457444.5 Sa: 0.2997   Find_Orb
M 359.49471 +/- 0.007
n 0.00294978 +/- 4.49e-5   Peri. 66.70168 +/- 0.010
a 48.1513817 +/- 0.488   Node 178.10801 +/- 0.0022
e 0.9373479 +/- 0.000631   Incl. 129.84837 +/- 0.0027
P 334.13   H 16.3 G 0.15 U 6.0
q 3.01678465 +/- 0.00024   Q 93.2859788 +/- 1.01
From 46 observations 2016 Jan. 8-Feb. 26; mean residual 0".33

1601 08.539167	F51	12 33 05.380	+11 34 34.72	.18-	.12+
1601 08.550115	F51	12 33 05.208	+11 34 45.68	.14-	.07+
1601 08.561083	F51	12 33 05.036	+11 34 56.59	.10-	.05-
1601 09.539670	F51	12 32 49.585	+11 51 28.37	.26+	.09-
1601 09.552913	F51	12 32 49.347	+11 51 42.32	.14+	.28+
1601 09.555566	F51	12 32 49.303	+11 51 44.76	.17+	.00
1601 09.566197	F51	12 32 49.099	+11 51 55.60	.10-	.07-
1601 09.568824	F51	12 32 49.074	+11 51 58.04	.21+	.32-
1601 09.579430	F51	12 32 48.874	+11 52 08.95	.00	.30-
1601 09.582057	F51	12 32 48.839	+11 52 12.01	.17+	.07+
1602 04.49426	F51	12 16 04.78	+21 12 32.8	.50-	.05+
1602 04.50808	F51	12 16 03.88	+21 12 54.4	.39-	.09+
1602 04.52186	F51	12 16 02.99	+21 13 16.2	.17-	.39+
1602 14.44094	F51	12 03 29.862	+25 42 34.35	.11+	.35-
1602 14.45270	F51	12 03 28.799	+25 42 54.56	.13-	.02-
1602 14.46446	F51	12 03 27.771	+25 43 14.54	.11+	.09+
1602 15.33470	291	12 02 10.60	+26 07 43.5	.46+	.04+
1602 15.33798	291	12 02 10.27	+26 07 49.3	.04+	.28+

Figure 22: Find_Orb data for P10sJtm before, with, and after my observations

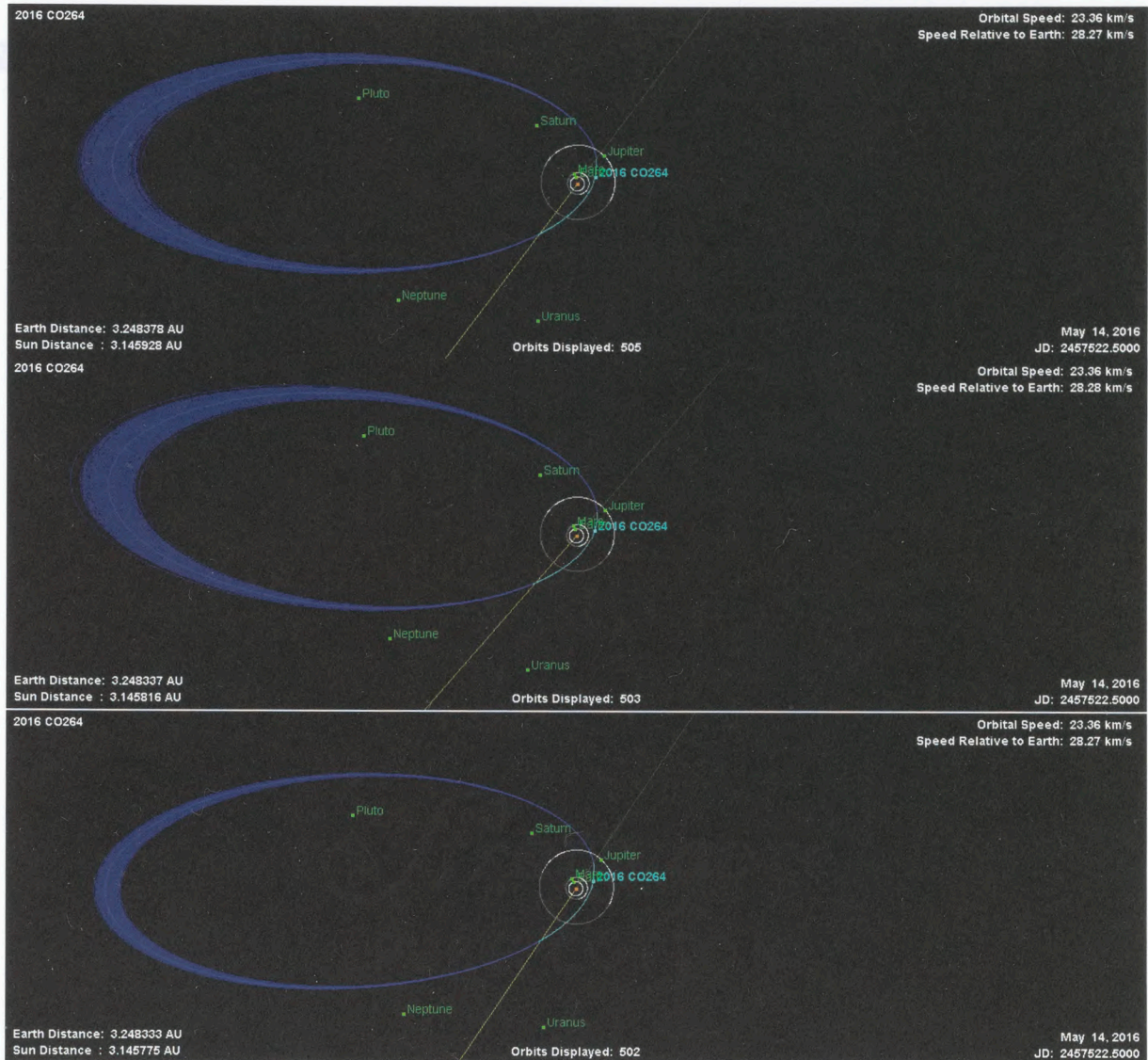Figure 23: OrbitMaster visualizations for P10sJtm before, with, and after my observations

2012 SZ₅₈

Orbital elements: 2012 SZ58
Perihelion 2012 Nov 17.785236 +/- 0.0101 TT = 18:50:44 (JD 2456249.285238
Epoch 2012 Dec 14.0 TT = JDT 2456275.5 Earth MOID: 0.6564 Find_Orb
M 10.18583 +/- 0.0038
n 0.38855354 +/- 5.15e-6   Peri. 76.31379 +/- 0.006
a 1.85995367 +/- 1.64e-5   Node 330.26896 +/- 0.0007
e 0.1511806 +/- 2.75e-6   Incl. 15.57719 +/- 0.00020
P 2.54/926.50d   H 18.3 G 0.15 U 4.6
q 1.57876468 +/- 1.16e-5 Q 2.14114267 +/- 2.23e-5
From 48 observations 2012 Sept. 27-Dec. 14; mean residual 0".43

1210 22.80890	461	01 12 23.99	+45 32 54.3	.10-	.10-
1211 08.21090	704	00 49 18.81	+45 09 59.1	.00	.44+
1211 08.22576	704	00 49 17.85	+45 09 54.1	.25+	.86+
1211 08.24122	704	00 49 16.74	+45 09 47.5	.68-	.03-
1211 08.25609	704	00 49 15.77	+45 09 42.0	.59-	.04+
1211 08.27118	704	00 49 14.84	+45 09 36.5	.04+	.26+
1211 10.14232	704	00 47 30.72	+44 57 39.1	.32+	.19-
1211 10.15688	704	00 47 29.84	+44 57 33.8	.02+	.24+
1211 10.17160	704	00 47 29.01	+44 57 27.7	.36+	.01+
1211 10.18671	704	00 47 28.16	+44 57 21.6	.74+	.00
1212 10.15441	703	00 51 56.01	+40 23 04.5	.58+	1.0-
1212 10.16118	703	00 51 56.30	+40 23 02.1	.71-	.31+
1212 10.16791	703	00 51 56.73	+40 22 57.9	.38-	.19-
1212 10.17468	703	00 51 57.16	+40 22 54.4	.08-	.03+
1212 14.068979	H21	00 56 31.81	+39 48 52.6	.05+	.08+
1212 14.071970	H21	00 56 32.01	+39 48 51.1	.12-	.11+
1212 14.074895	H21	00 56 32.29	+39 48 49.5	.69+	.01+
1212 14.077489	H21	00 56 32.41	+39 48 48.3	.08-	.14+

Orbital elements: 2012 SZ58
Perihelion 2015 Jun 2.158753 +/- 0.00533 TT = 3:48:36 (JD 2457175.658753)
Epoch 2016 Feb 4.0 TT = JDT 2457422.5 Earth MOID: 0.6570 Find_Orb
M 95.89681 +/- 0.0022
n 0.38849589 +/- 7.6e-7   Peri. 76.31280 +/- 0.0020
a 1.86013768 +/- 2.43e-6   Node 330.25506 +/- 0.00018
e 0.1509339 +/- 1.59e-6   Incl. 15.57889 +/- 0.000036
P 2.54/926.63d   H 18.2 G 0.15 U 3.4
q 1.57937978 +/- 1.99e-6 Q 2.14089558 +/- 5.36e-6
From 54 observations 2012 Sept. 27-2016 Feb. 4; mean residual 0".43

1211 08.27118	704	00 49 14.84	+45 09 36.5	.06+	.38+
1211 10.14232	704	00 47 30.72	+44 57 39.1	.32+	.07-
1211 10.15688	704	00 47 29.84	+44 57 33.8	.02+	.36+
1211 10.17160	704	00 47 29.01	+44 57 27.7	.36+	.13+
1211 10.18671	704	00 47 28.16	+44 57 21.6	.73+	.12+
1212 10.15441	703	00 51 56.01	+40 23 04.5	.52+	1.1-
1212 10.16118	703	00 51 56.30	+40 23 02.1	.77-	.18+
1212 10.16791	703	00 51 56.73	+40 22 57.9	.44-	.33-
1212 10.17468	703	00 51 57.16	+40 22 54.4	.14-	.10-
1212 14.068979	H21	00 56 31.81	+39 48 52.6	.03+	.11-
1212 14.071970	H21	00 56 32.01	+39 48 51.1	.14-	.08-
1212 14.074895	H21	00 56 32.29	+39 48 49.5	.67+	.18-
1212 14.077489	H21	00 56 32.41	+39 48 48.3	.10-	.05-
1602 03.71865	323	11 54 57.43	-03 52 37.2	.11+	.09+
1602 03.73664	323	11 54 56.67	-03 52 46.3	.14-	.10+
1602 03.75443	323	11 54 55.98	-03 52 55.7	.57+	.31-
1602 04.71588	323	11 54 17.44	-04 00 55.0	.24-	.57+
1602 04.73359	323	11 54 16.71	-04 01 04.1	.47+	.25+

Orbital elements: 2012 SZ58
Perihelion 2015 Jun 2.175110 +/- 0.00277 TT = 4:12:09 (JD 2457175.675110)
Epoch 2016 Mar 11.0 TT = JDT 2457458.5 Earth MOID: 0.6569 Find_Orb
M 109.87592 +/- 0.0011
n 0.38849454 +/- 4.18e-7   Peri. 76.31598 +/- 0.0009
a 1.86014200 +/- 1.34e-6   Node 330.25480 +/- 0.00007
e 0.1509649 +/- 1.31e-6   Incl. 15.57852 +/- 0.000032
P 2.54/926.64d   H 18.0 G 0.15 U 2.9
q 1.57932578 +/- 1.78e-6 Q 2.14095822 +/- 3.7e-6
From 75 observations 2012 Sept. 27-2016 Mar. 11; mean residual 0".39

1212 14.077489	H21	00 56 32.41	+39 48 48.3	.12-	.05-
1602 03.71865	323	11 54 57.43	-03 52 37.2	.03+	.06-
1602 03.73664	323	11 54 56.67	-03 52 46.3	.22-	.05-
1602 03.75443	323	11 54 55.98	-03 52 55.7	.50+	.46-
1602 04.71588	323	11 54 17.44	-04 00 55.0	.32-	.42+
1602 04.73359	323	11 54 16.71	-04 01 04.1	.39+	.10+
1602 04.75133	323	11 54 15.87	-04 01 13.4	.47-	.42-
1602 10.48350	F51	11 49 36.230	-04 45 28.33	.01+	.25+
1602 10.48414	F51	11 49 36.192	-04 45 28.61	.00	.24+
1602 10.49458	F51	11 49 35.571	-04 45 33.17	.06-	.17+
1602 10.49523	F51	11 49 35.539	-04 45 33.37	.04+	.25+
1602 10.50568	F51	11 49 34.919	-04 45 37.87	.01+	.24+
1602 10.50632	F51	11 49 34.873	-04 45 38.18	.11-	.20+
1602 10.51675	F51	11 49 34.266	-04 45 42.67	.06+	.19+
1602 10.51740	F51	11 49 34.228	-04 45 42.93	.06+	.21+
1602 29.40952	F51	11 25 49.784	-06 21 58.67	.02+	.01+

Figure 24: Find_Orb data for 2012 SZ58 before, with, and after my observations

Figure 25: OrbitMaster visualizations for 2012 SZ₅₈ before, with, and after my observations preceded by a zoomed out "before" visual which is indiscernible from the "with" & "after" visualizations

2012 BC₂

Figure 25: OrbitMaster visualizations for 2012 SZ$_{58}$ before, with, and after my observations preceded by a zoomed out "before" visual which is indiscernible from the "with" &"after" visualizations.
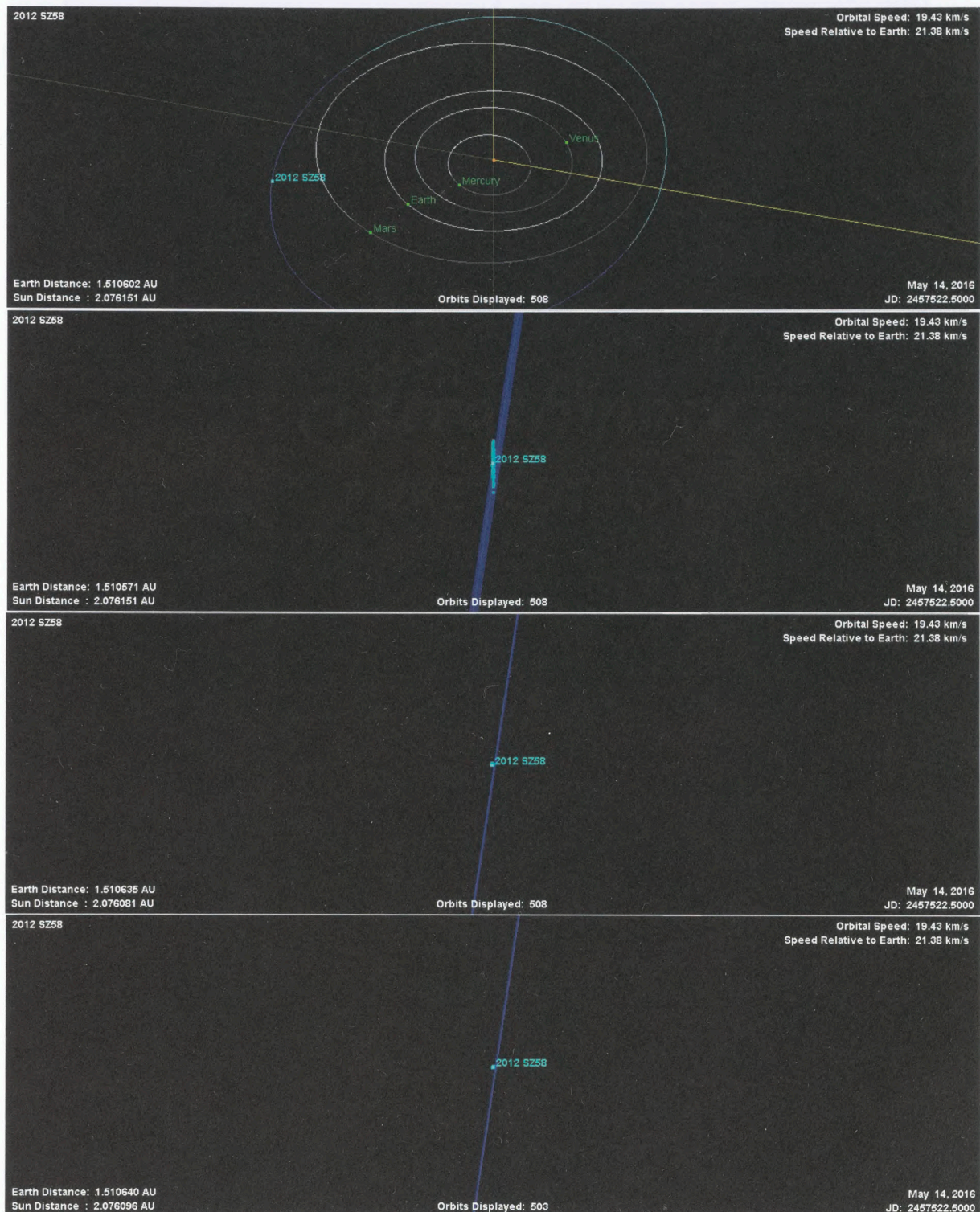
2012 BC$_3$

Orbital elements: 2012 BC3
Perihelion 2016 Jun 7.815441 +/- 0.000808 TT = 19:34:14 (JD 2457547.31544
Epoch 2016 Mar 7.0 TT = JDT 2457454.5   Find_Orb
M 338.44051 +/- 0.00017
n 0.23228337 +/- 9.24e-8   Peri. 23.52943 +/- 0.00012
a 2.62094133 +/- 6.95e-7   Node 128.50866 +/- 0.000059
e 0.1961139 +/- 2.16e-6   Incl. 14.63275 +/- 0.00006
P 4.24   H 17.0 G 0.15 U 1.9
q 2.10693818 +/- 6.2e-6   Q 3.13494449 +/- 4.89e-6
From 51 observations 2011 Dec. 25-2016 Mar. 7; mean residual 0".41

1202 22.25007	703	09 37 06.20	+22 45 08.0	.07+	.14-
1202 22.25885	703	09 37 05.77	+22 45 13.9	.18-	.77-
1202 22.26768	703	09 37 05.30	+22 45 21.3	.95-	.07+
1202 22.27650	703	09 37 04.94	+22 45 27.4	.20-	.37-
1202 29.20952	703	09 32 21.66	+24 04 47.9	.43+	.58-
1202 29.21566	703	09 32 21.30	+24 04 51.8	1.1-	.58-
1202 29.22189	703	09 32 21.19	+24 04 55.5	.75+	.82-
1202 29.22807	703	09 32 20.90	+24 05 00.6	.16+	.36+
1408 22.52860	F51	00 23 03.382	-12 43 15.41	.14+	.28-
1408 22.53976	F51	00 23 03.070	-12 43 20.87	.09+	.07+
1408 22.55094	F51	00 23 02.753	-12 43 26.91	.02-	.15-
1408 23.54528	F51	00 22 36.252	-12 52 06.67	.10+	.17+
1408 23.55802	F51	00 22 35.868	-12 52 13.53	.14-	.02-
1408 23.57073	F51	00 22 35.502	-12 52 20.13	.13-	.04+
1602 04.02399	807	06 10 14.54	+15 46 42.7	.04+	.19+
1602 04.02990	807	06 10 14.41	+15 46 45.8	.04+	.27-
1602 04.03584	807	06 10 14.28	+15 46 49.3	.05+	.34-
1603 07.09865	754	06 17 52.03	+20 31 50.9	.10+	.25-

Orbital elements: 2012 BC3
Perihelion 2016 Jun 7.735634 +/- 0.0343 TT = 17:39:18 (JD 2457547.235634)
Epoch 2014 Aug 23.0 TT = JDT 2456892.5   Find_Orb
M 207.95700 +/- 0.0058
n 0.23222043 +/- 3.2e-6   Peri. 23.45721 +/- 0.0044
a 2.62141484 +/- 2.41e-5   Node 128.51020 +/- 0.00012
e 0.1958192 +/- 6.01e-6   Incl. 14.63296 +/- 0.00014
P 4.24   H 16.9 G 0.15 U 4.3
q 2.10809131 +/- 8.58e-6   Q 3.13473837 +/- 4.35e-5
From 46 observations 2011 Dec. 25-2014 Aug. 23; mean residual 0".43

1201 31.43363	703	09 53 13.52	+17 42 32.7	.17+	.11+
1202 15.34815	F51	09 42 21.746	+21 14 58.36	.10+	.25+
1202 15.36201	F51	09 42 21.059	+21 15 09.81	.08+	.20+
1202 15.37588	F51	09 42 20.368	+21 15 21.29	.03+	.20+
1202 15.38983	F51	09 42 19.680	+21 15 32.89	.11+	.27+
1202 22.25007	703	09 37 06.20	+22 45 08.0	.02+	.14-
1202 22.25885	703	09 37 05.77	+22 45 13.9	.23-	.77-
1202 22.26768	703	09 37 05.30	+22 45 21.3	1.0-	.07+
1202 22.27650	703	09 37 04.94	+22 45 27.4	.25-	.38-
1202 29.20952	703	09 32 21.66	+24 04 47.9	.37+	.59-
1202 29.21566	703	09 32 21.30	+24 04 51.8	1.2-	.58-
1202 29.22189	703	09 32 21.19	+24 04 55.5	.70+	.83-
1202 29.22807	703	09 32 20.90	+24 05 00.6	.10+	.36+
1408 22.52860	F51	00 23 03.382	-12 43 15.41	.16+	.35-
1408 22.53976	F51	00 23 03.070	-12 43 20.87	.11+	.00
1408 22.55094	F51	00 23 02.753	-12 43 26.91	.00	.22-
1408 23.54528	F51	00 22 36.252	-12 52 06.67	.12+	.09+
1408 23.55802	F51	00 22 35.868	-12 52 13.53	.11-	.09-

Figure 26: Find_Orb data for 2012 BC$_3$ before and with my observations. My observations are the most recent observations so there is no "after" to show.

Figure 27: OrbitMaster visualizations for 2012 BC3 before and with my observations. The first image simply shows a zoomed out image of the orbit.
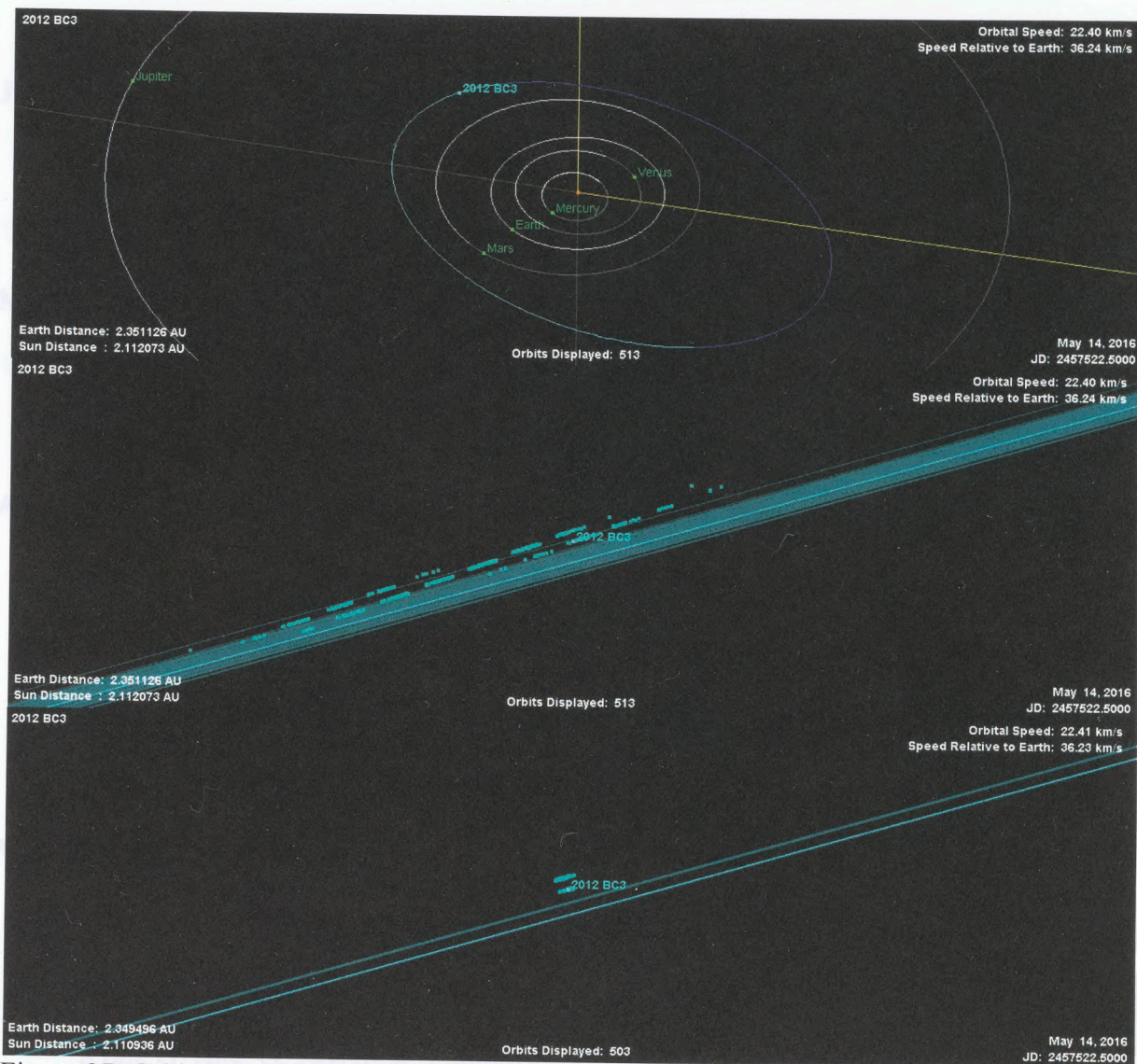
Figure 27: OrbitMaster visualizations for 2012 BC3 before and with my observations. The first image simply shows a zoomed out image of the orbit.

References

J. Biggs, A. W. Puckett, J. E. Brown, V. L. Hoette, R. Groom, K. Stranger, A. L. Caughey, N. E. Garcia, X. P. Lopez, D. D. Webb, B. A. O'Keeffe, "Minor Planet Observations [323 Perth Observatory, Bickley]", *Minor Planet Circ.*, **97718**, 1 (2016).

M. W. Buie, D. Wittman, L. H. Wasserman, R. Holmes, A. W. Puckett, T. R. Linder, L. Buzzi, A. L. Caughey, V. L. Hoette, "Minor Planet Observations [807 Cerro Tololo]", *Minor Planet Circ.*, **98868**, 4 (2016).

A. L. Caughey, R. Groom, K. Stranger, A. W. Puckett, A. C. Gilmore, P. M. Kilmartin, M. Schwartz, P. R. Holvorcem, D. C. Fuls, A. D. Grauer, E. J. Christensen, A. R. Gibbs, J.A. Johnson, R. A. Kowalski, S. M. Larson, G. J. Leonard, R. G. Matheny, R. L. Seaman, F. C. Shelly, W. H. Ryan, E. V. Ryan, , "2016 CD$_{137}$", *Minor Planet Electronic Circ.*, **2016-C120** (2016).

A. L. Caughey, R. Groom, K. Stranger, A. W. Puckett, M. Schwartz, P. R. Holvorcem, A. D. Grauer, E. J. Christensen, D. C. Fuls, A. R. Gibbs, J. A. Johnson, R. A. Kowalski, S. M. Larson, G. J. Leonard, R. G. Matheny, R. L. Seaman, F. C. Shelly, W. H. Ryan, E. V. Ryan, G. Hug, G. Favero, R. Furgoni, "2016 CL$_{137}$", *Minor Planet Electronic Circ.*, **2016-C129** (2016).

M. Connors, A. L. Caughey, A. W. Puckett, V. L. Hoette, I. Schofield, N. E. Garcia, X. P. Lopez, D. D. Webb, B. A. O'Keeffe, "Minor Planet Observations [U96 Athabasca University Geophysical Observatory, Athabasca]", *Minor Planet Circ.*, **98485**, 2 (2016).

A. C. Gilmore, P. M. Kilmartin, J. A. Johnson, E. J. Christensen, D. C. Fuls, A. R. Gibbs, A. D. Grauer, R. A. Kowalski, S. M. Larson, G. J. Leonard, R. G. Matheny, R. L. Seaman, F.

C. Shelly, M. Schwartz, P. R. Holvorcem, A. Hidas, V. L. Hoette, R. Treffers, R. L. Sanchez, A. L. Caughey, A. W. Puckett, T. R. Linder, W. H. Ryan, E. V. Ryan, "2016 CH$_{137}$", *Minor Planet Electronic Circ.*, **2016-C124** (2016).

B. Gray, 2016, Find_Orb Orbit Determination Software, v 3 Jan 2016, Project Pluto, http://www.projectpluto.com/find_orb.htm

V. L. Hoette, D. Gray, J. Haislip, E. Struble, A. L. Caughey, A. W. Puckett, T. R. Linder, R. Holmes, T. A. Rector, L. Franklin, V. Goss, J. Jensen, K. Bakker, J. C. Campbell, C. Fielding, B. Konstantynowicz, K. Miller, S. Nichols, A. Blalock, P. Carter-Amorin, M. Odom, K. Huynh, S. Bin Zubaeir, M. Evenson, H. Greiner, K. Pritchard, D. Sobek, C. Reed, B. Rosin, T. Weissler, T. Wagoner, L. Brown, D. Houser, A. Natalroman, C. Yang, N. Qureshi, S. Samson, N. Spencer, J. Thornton, S. Wright, E. Zwiacher, K. Gibertoni, H. Lindsey, M. Valdez, T. Zimmerman, M. Alvarenga-Gaxiola, A. Davis, M. Brown, S. Friess, S. Graper, M. Pyhala, B. Edwards, E. B. Edwards, M. Helveston-Larson, Y. Olidan, C. Powers, A. Raszewski, A. Taylor, R. L. Sanchez, K. Kade, A. Nugent, D. Smith, S. Forrest, T. W. Clason, "Minor Planet Observations [754 Yerkes Observatory, Williams Bay]", *Minor Planet Circ.*, **98868**, 3 (2016).

M. Krolikowska, G. Sitarski, A. M. Soltan, "How selecting and weighing of astrometric observations influence the impact probability. The case of asteroid (99942) Apophis", *Monthly Notices of the Royal Astronomical Society*, Vol. 399, Issue 4, pp. 1964-1976 2009, doi:10.1111/j.1365-2966.2009.15276.x

G. J. Leonard, E. J. Christensen, D. C. Fuls, A. R. Gibbs, A. D. Grauer, J. A. Johnson, R. A. Kowalski, S. M. Larson, R. G. Matheny, R. L. Seaman, F. C. Shelly, J. Jahn, B. Gibson, T. Goggia, N. Primak, A. Schultz, M. Willman, K. Chambers, S. Chastel, L. Denneau, H.

Flewelling, M. Huber, E. Lilly, E. Magnier, R. Wainscoat, C. Waters, R. Weryk, P. Veres, T. Felber, V. L. Hoette, R. Treffers, A. W. Puckett, T. R. Linder, R. L. Sanchez, A. L. Caughey, W. H. Ryan, E. V. Ryan, M. Suzuki, "2016 CM$_{194}$", *Minor Planet Electronic Circ.,* **2016-C160** (2016).

R. A. Mastaler, J. V. Scotti, R. J. Wainscoat, C. Wipper, M. Micheli, J. V. Scotti, K. Nault, M. Hammergren, M. Brucker, J. G. Ries, V. L. Hoette, A. W. Puckett, A. L. Caughey, R. L. Sanchez, T. R. Linder, B. Gibson, T. Goggia, N. Primak, A. Schultz, M. Willman, K. Chambers, S. Chastel, L. Denneau, H. Flewelling, M. Huber, E. Lilly, E. Magnier, R. Wainscoat, C. Waters, R. Weryk, P. Veres, W. H. Ryan, E. V. Ryan, H. Sato, "2016 CO$_{264}$", *Minor Planet Electronic Circ.,* **2016-D46** (2016).

N. Metropolis, S. Ulam, "The Monte Carlo Method", *Journal of the American Statistical Association*, Vol. 44, No. 247, Sept 1949, pp. 335-341.

H. Raab, 2015, Astrometrica, v4.9.1.420, http://www.astrometrica.at/

D. E. Reichart, J. B. Haislip, K. M. Ivarsen, J. A. Crain, A. C. Foster, 2016, Skynet Robotic Telescope Network, https://skynet.unc.edu/

A.W. Puckett, T.A. Rector, R. Baalke, O. Ajiki, "OrbitMaster: An Online Tool for Investigating Solar System Dynamics and Visualizing Orbital Uncertainties in the Undergraduate Classroom", AAS Meeting Abstracts, **227**, 328.09, (2016).

DATE DUE

PRINTED IN U.S.A.